



6-Fluorophenylbenzohydrazides inhibit *Mycobacterium tuberculosis* growth through alteration of tryptophan biosynthesis



Sara Consalvi ^{a,1}, Giulia Venditti ^{a,1}, Junhao Zhu ^b, Helena I. Boshoff ^c, Kriti Arora ^c, Alessandro De Logu ^d, Thomas R. Ioerger ^e, Eric J. Rubin ^b, Mariangela Biava ^a, Giovanna Poce ^{a,*}

^a Department of Chemistry and Technologies of Drug, Sapienza University of Rome, Piazzale A. Moro 5, 00185, Rome, Italy

^b Department of Immunology and Infectious Diseases, Harvard T.H. Chan School of Public Health, 677 Huntington Avenue, Boston, MA, 02115, USA

^c National Institute of Allergy and Infectious Diseases, Laboratory of Clinical Immunology and Microbiology, 9000 Rockville Pike, Bethesda, MD, 20892, USA

^d Department of Life and Environmental Sciences, University of Cagliari, via Ospedale 72, 09124, Cagliari, Italy

^e Department of Computer Science, Texas A&M University, 3112 TAMU, College Station, TX, 77843, USA

ARTICLE INFO

Article history:

Received 14 July 2021

Received in revised form

31 August 2021

Accepted 7 September 2021

Keywords:

6-Fluorophenylbenzohydrazides

Drug development

Tryptophan biosynthesis

Tuberculosis

ABSTRACT

A major constraint in reducing tuberculosis epidemic is the emergence of strains resistant to one or more of clinically approved antibiotics, which emphasizes the need of novel drugs with novel targets. Genetic knockout strains of *Mycobacterium tuberculosis* (*Mtb*) have established that tryptophan (Trp) biosynthesis is essential for the bacterium to survive *in vivo* and cause disease in animal models. An anthranilate-like compound, **6-FABA**, was previously shown to synergize with the host immune response to *Mtb* infection *in vivo*. Herein, we present a class of anthranilate-like compounds endowed with good antimycobacterial activity and low cytotoxicity. We show how replacing the carboxylic moiety with a hydrazide led to a significant improvement in both activity and cytotoxicity relative to the parent compound **6-FABA**. Several new benzohydrazides (compounds **20–31**, **33**, **34**, **36**, **38** and **39**) showed good activities against *Mtb* ($0.625 \leq \text{MIC} \leq 6.25 \mu\text{M}$) and demonstrated no detectable cytotoxicity against Vero cell assay ($\text{CC}_{50} \geq 1360 \mu\text{M}$). The target preliminary studies confirmed the hypothesis that this new class of compounds inhibits Trp biosynthesis. Taken together, these findings indicate that fluoro-phenylbenzohydrazides represent good candidates to be assessed for drug discovery.

© 2021 Elsevier Masson SAS. All rights reserved.

1. Introduction

Despite decades of global efforts in combatting tuberculosis (TB), it remained one of the world's leading causes of death from a single infectious agent, accounting for over one million deaths annually [1]. A major constraint in controlling TB has been the rise of multidrug-resistant TB (MDR-TB), and extensively drug-resistant TB (XDR-TB), both of which impedes the application of conventional antitubercular antibiotic, emphasizing the need for new drugs against novel targets.

The concern that host metabolites could rescue inhibition of enzymes in amino acid biosynthesis in pathogens with an

intracellular lifestyle like *Mycobacterium tuberculosis* (*Mtb*), is counteracted by studies that demonstrated the essentiality of many of the enzymes involved in amino acid biosynthesis for survival in nutrient-limited environments such as in the host [2–4] reinforcing the notion that these are potentially attractive drug targets. However, these pathways have largely remained unexplored from a drug target perspective. Moreover, inhibitors of *Mtb* biosynthetic pathways may show selective toxicity because many amino acids are classified as essential in humans and lack human orthologues.

There is a growing interest in studying mycobacterial tryptophan (Trp) biosynthesis and its critical role in counteracting host immune responses upon *Mtb* infection [5]. Tryptophan-auxotrophic *Mtb* strains lacking either *trpE*, *trpD* or *trpA* showed reduced survival and failed to cause disease in both immunocompetent and immunocompromised mice [2,6,7]. *Mtb*'s specific demand for *de novo* Trp biosynthesis during infection is likely due to host-mediated Trp deprivation: upon infection, activated

* Corresponding author.

E-mail addresses: mariangela.biava@uniroma1.it (M. Biava), giovanna.poce@uniroma1.it (G. Poce).

¹ S. Consalvi and G.Venditti contributed equally to the work.

macrophages express indoleamine 2,3-dioxygenase (IDO), which catabolizes Trp to kynureine and potentially starves intracellular *Mtb* of extracellular Trp. This model is corroborated by clinical studies whereby elevated levels of IDO transcripts were found in sputum samples collected from a cohort of TB patients [8], as well as in blood cells of active or latent TB (LTBI) patients [9]. In addition to deprivation of intracellular Trp pool, IDO-mediated Trp catabolism was shown to induce immune tolerance by modulating the CD4⁺ T cell response [10]. Together, these data suggest that the human immune system is proficient at depleting intramacrophagal Trp pool to restrict *Mtb* growth, the effect of which could therefore be intensified by the selective disruption of mycobacterial Trp biosynthesis.

Indeed, previous works suggest that alteration of Trp biosynthesis by an anthranilate-like compound (**6-FABA**, Fig. 1) synergizes with the host immune response to *Mtb* infection *in vivo*. **6-FABA** showed a minimum inhibitory concentration (MIC) of 5 μ M in liquid broth in the absence of Trp, while the addition of Trp to the medium restored *Mtb* growth. When tested *in vivo* on a murine model of TB infection, **6-FABA** and its ethyl ester (Fig. 1) showed a significant reduction in bacterial load in infected mouse spleens (10-fold reduction respect to control) [6].

These intriguing data prompted us to develop this class of anthranilate-like compounds by designing new analogues that could show improved activity and mammalian cytotoxicity. In this study, we present our medicinal chemistry program including the design, synthesis, and profiling of a set of active analogues (**1–42**) and hypothesized that they cause functional Trp depletion in mycobacteria through the production of fluorinated Trp.

2. Results and discussion

2.1. Design strategy

Since carboxylate human/mammalian toxicity is related to the rearrangement of acyl glucuronides that can be produced *in vivo* and that can lead to chemically reactive species [11,12], we firstly focused on the replacement of the carboxylic group with either hydroxamic acid or hydroxamic acid methyl ester (compounds **1** and **2**, Fig. 2). Indeed, benzohydroxamic acids and esters are excellent bioisosteres of anthranilic acids, due to the resistance to metabolism and improved water solubility [13]. Moreover, oxadiazoles and tetrazoles as bioisosteres were incorporated in the place of carboxylate (**3–5**), since their acidity and planarity are comparable to those of carboxylic acids.

The most common approach to mask carboxylic acids is to prepare ester-based prodrugs that can also improve solubility, stability and oral bioavailability of small-molecule drugs [14]. However, the rapid bioconversion by esterases could release an excessive amount of acid in the serum, causing toxic effects attributed to the free carboxylic moiety. Therefore, we decided to prepare two subsets of derivatives replacing the ester group of the **6-FABA** ethyl ester with amides and hydrazides to improve the metabolic liabilities. In the frame of a thorough structure-activity

relationship (SAR) study, we synthesized different alkyl and aryl amides (**6–16**, Fig. 3) and hydrazides (**17–37**, Fig. 4). Finally, 2 aryl hydrazide hydrochlorides were prepared to improve aqueous solubility (**38** and **39**, Fig. 4).

In addition to the previous subsets of compounds, we included three trifluoromethyl amine derivatives (**40–42**, Fig. 5). Amide-bond substitution by trifluoroethylamine surrogates have been shown to grant metabolic stability, low basicity and ability to form hydrogen bonds [15].

Hydroxamates **1** and **2**, amides **6–16** and hydrazides **18–39** were prepared as shown in Scheme 1. **6-FABA** was activated with 1,1'-carbonyldiimidazole **43** to achieve the isatoic anhydride **44**, which was coupled *in situ* with either the suitable hydroxylamines **45a,b** or amines **46a-k** or hydrazines **47a-t** to afford the corresponding final compounds **1**, **2**, **6–16** and **18–37**. Finally, compounds **20** and **21** were converted into the corresponding hydrochloride salts **38** and **39** by reaction with HCl in ethanol.

Reagents and conditions: i) THF, rt, 24 h; ii) THF, rt, 15 h, yield 12–70%, %; iii) HCl 37%, ethanol, rt, 30 min, yield 90%.

Oxadiazole **3** was obtained as reported in Scheme 2. Briefly, the reaction between the 2-amino-6-fluoro benzonitrile **48** and hydroxylamine hydrochloride **49** in basic conditions led to the formation of amidoxime **50**. The latter was then cyclized by using *tert*-butyl acetate **51** to afford compound **3**.

Reagents and conditions: i) KOH, MeOH, 4 h, yield 68%; ii) *t*-BuOK, *t*-BuOH, 100 °C, 1.5 h, yield 55%.

Compounds **4** and **17** were synthesized as reported in Scheme 3. Deprotection of **18** with trifluoroacetic acid gave hydrazide **17**, which was then cyclized with triethyl orthoacetate **52** to achieve the oxadiazole derivative **4**.

Reagents and conditions: i) TFA, DCM, rt, 30 min, yield >90%; ii) dioxane, 100 °C, 24 h, yield 24%.

Tetrazole **5** was obtained in one-step from the cyclization of 2-amino-6-fluoro benzonitrile **53** with sodium azide (Scheme 4).

Reagents and conditions: i) NH₄Cl, DMF, 120 °C, 24 h, yield 24%.

Finally, trifluoromethyl amines **40–42** were obtained as shown in Scheme 5. Starting from the benzyl bromide **54**, the benzyl alcohol **55** was prepared by nucleophilic substitution in basic conditions. Then, alcohol **55** was oxidized to the corresponding aldehyde **56**, which was used to synthesize the trifluoromethyl benzyl alcohol **57**. The hydroxyl group was transformed into the corresponding trifluoromethyl sulphonate **58**, to promote the further reaction with the appropriate amine and formation of intermediates **59a-c**. Finally, the nitro group was reduced with nickel chloride and sodium borohydride to give the final compounds **40–42**.

Reagents and conditions: i) CaCO₃, H₂O, dioxane, reflux, 16 h, yield 75%; ii) Dess-Martin periodinane, DCM, 0 °C, 30 min, yield 55%; iii) (CH₃)₃SiCF₃, TBAF, THF, 0 °C, 1 h, yield 35%; iv) (CF₃)(SO₂)₂O, 2,6-lutidine, DCM, 0 °C, 3 h, yield 30%; v) Amine, K₂CO₃, DCM, reflux, 16 h, yield 43%; vi) NiCl₂(6H₂O), NaBH₄, CH₃CN, rt, 30 min, yield 60%.

2.2. SAR analysis

Since *in vitro* antibiotic efficacy can vary unpredictably with growth conditions [16], compounds **1–42** were tested against *Mtb* H37Rv in three different media: Middlebrook 7H9/ADC/Tween 80, Gast Fe and Middlebrook 7H9/DPPC/casitone/Tyloxapol (Tx) (Table 1). Unlike the Middlebrook 7H9/ADC/Tw, Gast Fe and Middlebrook 7H9/DPPC/casitone/Tx media do not contain BSA. The concentration of free drug in the medium could be reduced by a possible BSA-drug interaction, decreasing the *in vitro* activity of drug [17]. Furthermore, Middlebrook 7H9/DPPC/casitone/Tx medium contains dipalmitoyl phosphatidyl choline as carbon source,

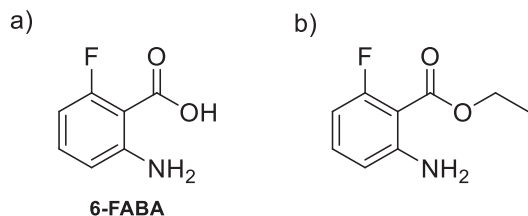


Fig. 1. a) Chemical structure of **6-FABA**; b) chemical structure of **6-FABA** ethyl ester.

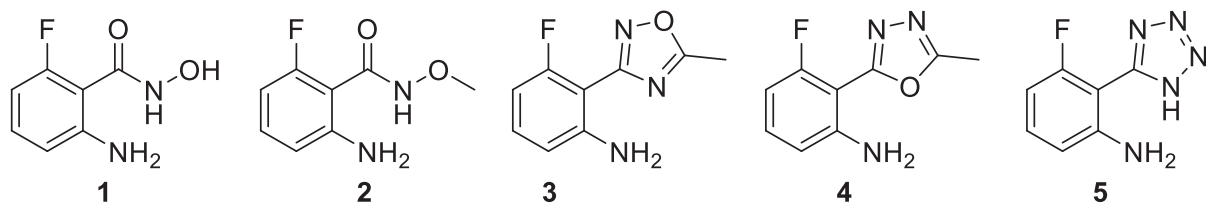


Fig. 2. Chemical structures of compounds 1–5.

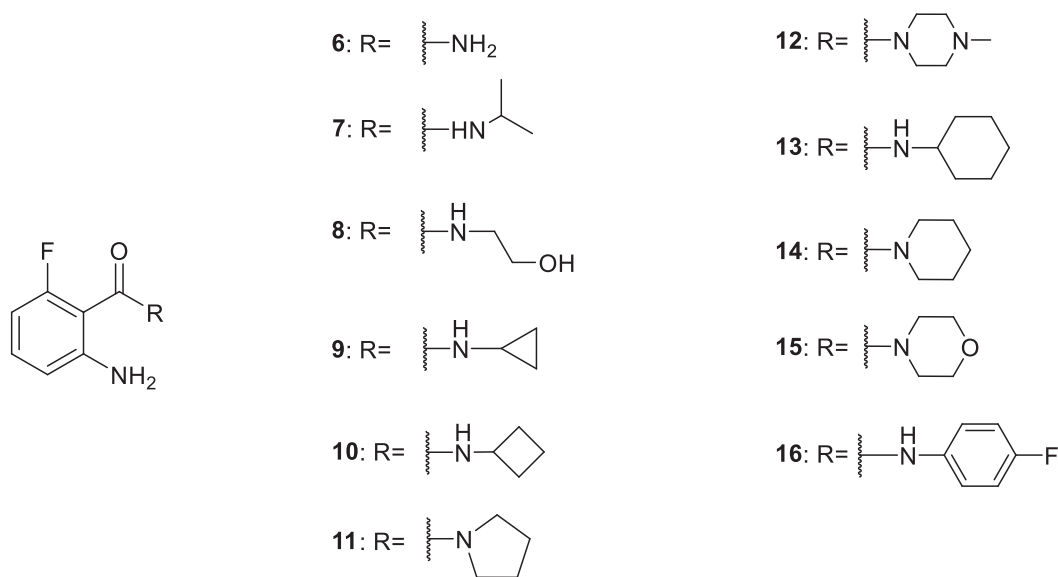


Fig. 3. Chemical structures of amides 6–16.

whereas the other two media contain glycolytic carbon sources (glucose and glycerol for 7H9/ADC/Tw and glycerol for Gast Fe) as well as oleic acid released by Tween 80 hydrolysis. Both glycolytic as well as beta-oxidation carbon sources support optimal growth of the pathogen *in vivo* depending on the host microenvironment as evidenced by the *in vivo* attenuation of Mtb mutants in glycolytic as well as gluconeogenic pathways [16]. The most active compounds (**19–29**, **31**, **33**, **34**, **36**, **38** and **39**) were evaluated for mammalian cytotoxicity by measuring the concentration of compound that causes a cytotoxic effect (CC_{50}) in 50% of treated Vero cells (Table 1).

Replacing the carboxylic group with either the hydroxamic acid or the hydroxamic ester group (compounds **1** and **2**, $MIC > 50 \mu M$) or the heterocyclic moieties (compounds **3–5**, $MIC > 50 \mu M$) led to a loss of activity. Likewise, the insertion of both amides (**6–16**) and trifluoromethyl amines (**40–42**) in the place of the ester functional group resulted in inactive compounds ($MIC > 50 \mu M$ in all media). Instead, among all the synthesized compounds only hydrazides **19–31**, **33**, **34**, **36**, **38** and **39** provided good growth inhibitory activity (Table 1). As expected, better results were obtained in cultures grown in both Middlebrook 7H9/DPPC/casitone/Tx and Gast Fe than those run in the Middlebrook 7H9/ADC/Tw one. Consistent with the previous speculations, BSA seems to negatively affect the anti-mycobacterial activity. Indeed, the significant lipophilicity of aryl hydrazides could promote the interaction with BSA, increasing the binding affinity. Among the hydrazides, the aromatic ones **20–31**, **33**, **34**, **36**, **38** and **39** stood out with good activities ($0.625 \leq MIC \leq 6.25 \mu M$, 7H9/DPPC/casitone/Tx). To date, the electronic effects of substituents on the hydrazide phenyl ring seem not to play a significant role on the activity. As general trend, *para*-

(**21**, **25**, **33** and **34**) and *meta*- (**22** and **24**) ($1.56 \mu M \leq MIC \leq 2.84 \mu M$, 7H9/DPPC/casitone/Tx) mono-substituted phenyl hydrazides are more active. Preparation of hydrochloride salts (**38** and **39**) of hydrazides **20** and **21** provided a significant improvement of the activity in all tested media (Table 1).

Potential mammalian toxicity of the hydrazides was one of our primary concerns since, as documented for isoniazid, the hydrazide moiety is often cause of production of toxic radical species [18]. To our satisfaction, active aryl hydrazides **20–31**, **33**, **34**, **36**, **38** and **39** demonstrated no detectable cytotoxicity against Vero cell assay ($CC_{50} \geq 1360 \mu M$) (Table 1).

2.3. Preliminary target studies

The FABAs compounds, as anthranilate analogues, possibly are, like other fluorinated anthranilates, antimetabolites altering tryptophan biosynthesis. The only well-characterized compound, **6-FABA**, appears to have a complex mechanism of action. Originally thought to be inhibitor of one of the early stages of Trp biosynthesis, either the formation of anthranilate by anthranilate synthetase (TrpE) or its modification by anthranilate phosphoribosyltransferase (TrpD) [6]. Subsequent work, however, made this less clear, its toxic mechanism, then, is downstream, either by inhibition of a subsequent step or through formation of fluoro-tryptophan and its incorporation into polypeptides [19,20].

2.3.1. Hydrazides cause distress in trp biosynthesis

Compounds presented in here could similarly act as substrates or could be inhibitors of either of the enzymes. To confirm that

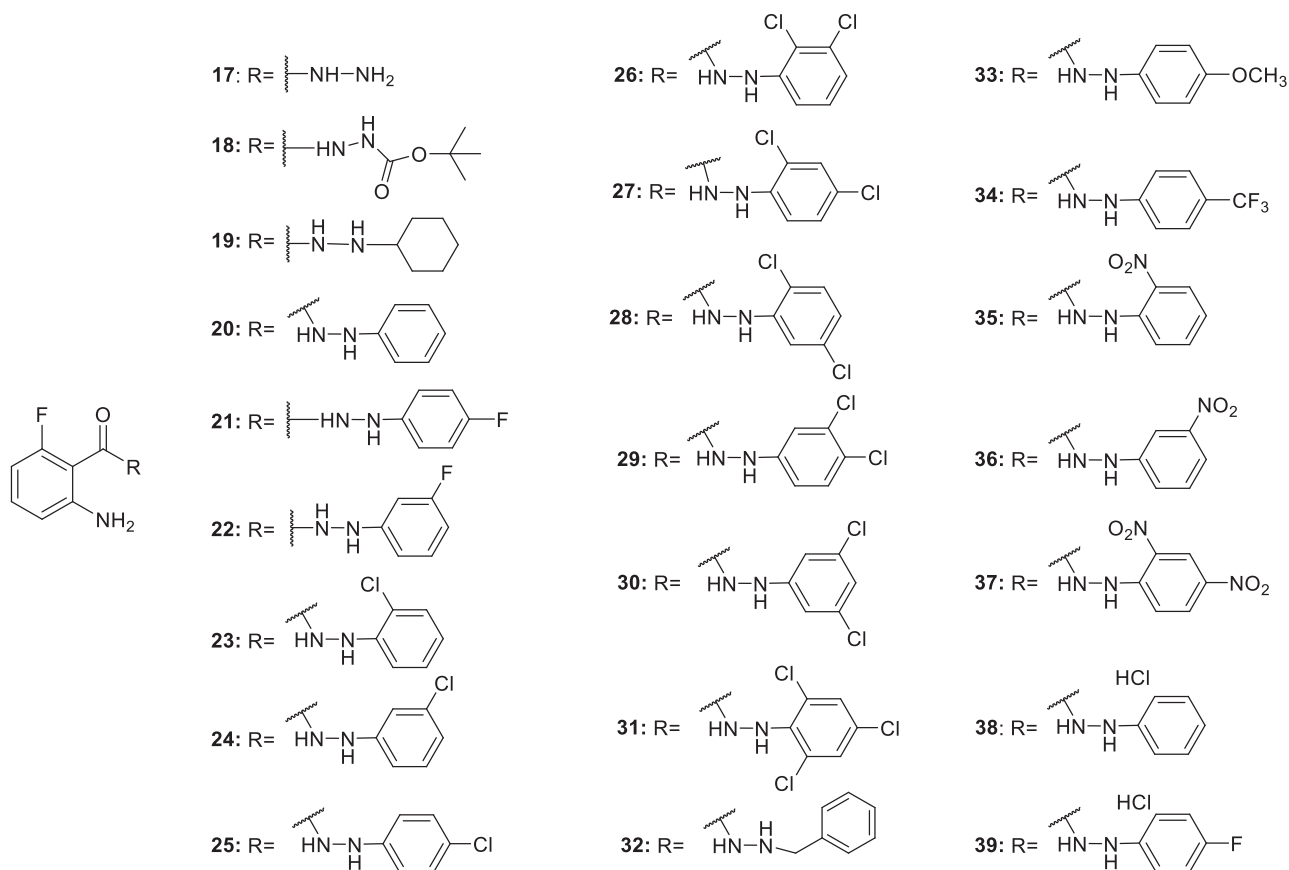


Fig. 4. Chemical structures of hydrazides 17–39.

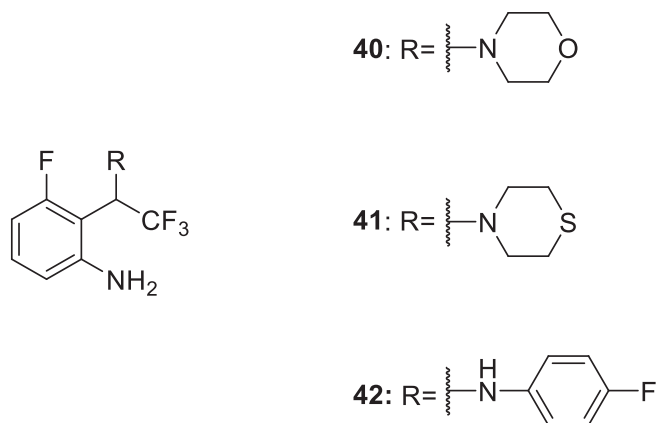


Fig. 5. Chemical structures of trifluoromethyl amines 40–42.

hydrazides exert their anti-mycobacterial activity via alteration of the mycobacterial Trp biosynthesis, hydrazide activities in the presence of Trp and its main biosynthesis precursors, chorismate, anthranilate and indole were assessed. A concentration of 0.1 mM of each precursor was added to a culture of BCG in 7H9/ADC/Tween 80 in the presence of **6-FABA** and hydrazides **20**, **31** and **38**. The addition of anthranilate, indole and Trp to cultures rescued BCG growth from the inhibitory activity of **6-FABA**, and hydrazides **20**, **31** and **38**, while cultures growth was inhibited in presence of chorismate (Table 2). Furthermore, repeating the test with an increased concentration of chorismate (0.5 mM) (Table 2), all the

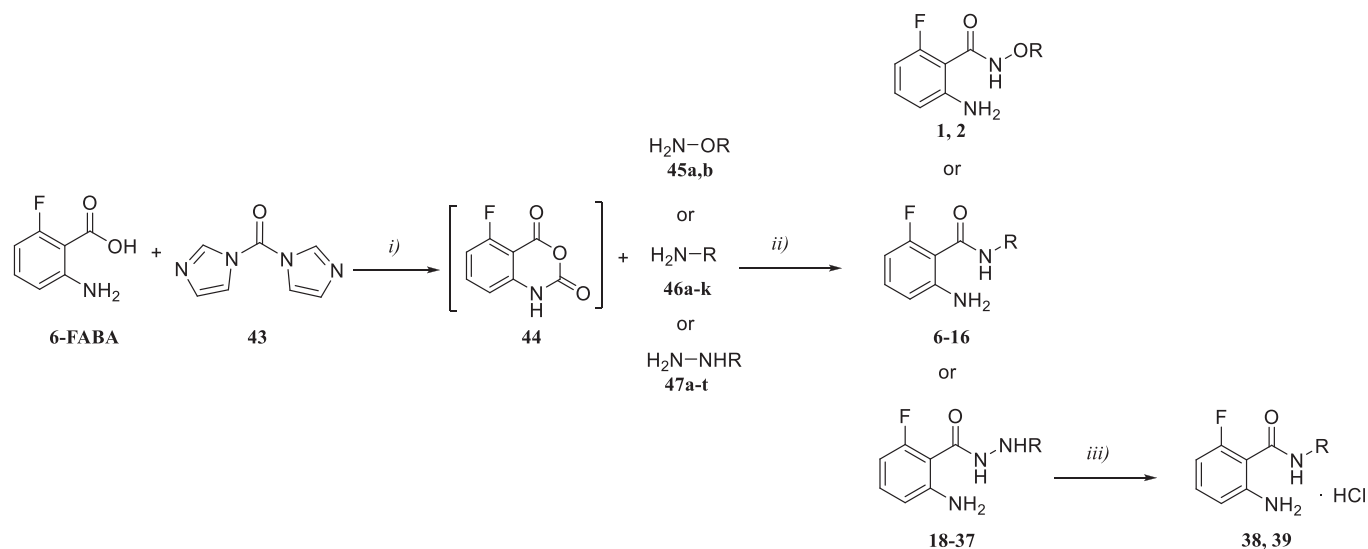
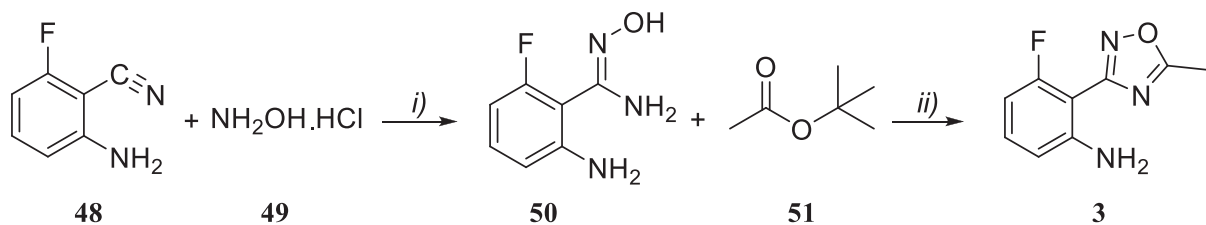
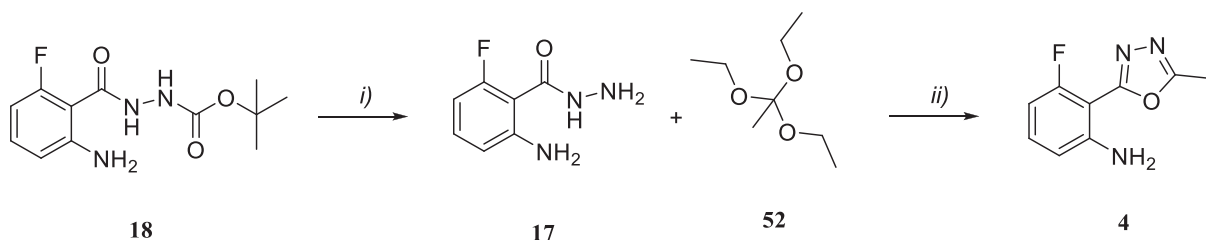
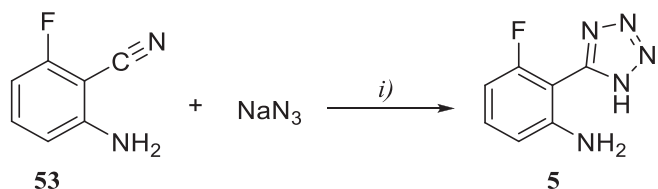
tested compounds proved to be still active. The ability of anthranilate, indole and Trp to rescue BCG from growth inhibition by these hydrazides suggests that they exert a pleiotropic effect on Trp biosynthesis.

2.3.2. Mutants resistant to hydrazides clustered into two groups

Consistent with the speculation that **6-FABA** and the new hydrazides act by inhibiting the same target, we expected to observe a cross-resistance between **38** and **6-FABA**. Therefore, **6-FABA** resistant mutants were generated to assess the activity of **38** against **6-FABA** resistors. Mycobacterial cultures ($OD_{600} = 0.4–0.5$) were plated onto solid media containing concentrations 5, 10, 20 times the *in vitro* MIC of **6-FABA** (Table 3). Resistors showing MICs 15-folds higher than the wild type strain were selected (Table 3) and displayed a lower sensitivity to **38**, compared to the wild-type, confirming the cross-resistance, indicating that **38** and **6-FABA** likely have the same mechanism.

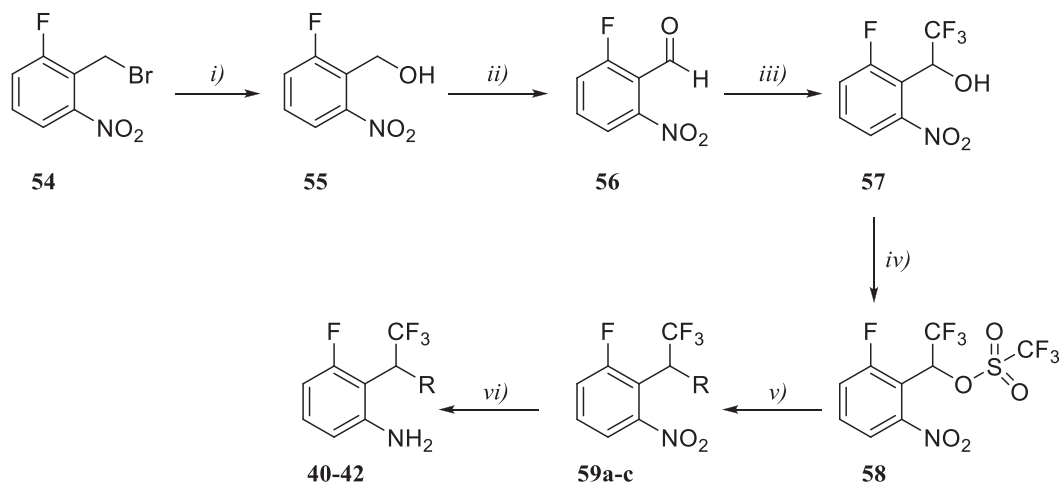
Considering the good toxicity/activity profile, compound **38** was chosen for the isolation and characterization of BCG resistant mutants. Mycobacterial cultures ($OD_{600} = 0.4–0.5$) were plated onto solid media containing concentrations 3, 5, 10 and 20 times the MIC of compound **38** (Table 4). Different resistor colonies were isolated with a frequency approximately of 3×10^{-4} . All the resistant mutants showed to lose susceptibility to **38**, with MICs 7-fold higher than to the wild type (Table 4). Moreover, **6-FABA** exhibited a lower activity on **38** resistors compared to those of the wild type. The genomic DNA of each resistor was extracted and sequenced. The resistors mutations are reported in Table 4 (see Table 5).

The relatively high frequency of spontaneous compound **38** resistant mutant formation ($\sim 3 \times 10^{-4}$) and the multi-gene

Scheme 1. Synthetic pathway for compounds **1**, **2**, **6-16** and **18-39**.Scheme 2. Synthetic pathway for compound **3**.Scheme 3. Synthetic pathway for compounds **4** and **17**.Scheme 4. Synthetic pathway for compound **5**.

mutational landscape of the isolated compound **38** resisters (Table 4) imply a complex resistance mechanism for compound **38**. Notably, 7 of the 9 resistant mutants had mutations in a gene in the Trp biosynthesis pathway, including TrpB, TrpC, TrpD, and TrpE. The fact that almost all resistant mutants have mutations in genes in this pathway strongly implicates interference with Trp synthesis as

the mechanism of action for **38**. However, the lack of a confined mutational "hot spot", as was found in many other compounds with reported inhibitory activities on tryptophan biosynthesis, implies that these *trp* mutations likely modulate the metabolic flux of the tryptophan biosynthesis pathway, rather than directly affecting the binding of compound **38** to its enzymatic target. 6 of the 7 mutations in Trp genes are non-synonymous substitutions. Of these, TrpC:V92A, TrpB:E225, and TrpD:T108 N are in their respective active sites, whereas, TrpE:P91H, TrpB:T198 N, and TrpB:A132V are not proximal to the active sites. However, it is well-known that TrpE/TrpG are allosterically-regulated [21,22], and allosteric inhibition of other enzymes in this pathway by other compounds has been observed [7,23], so these distal mutations could affect catalytic efficiency. Mutant 5 has a frame-shift mutation; however, it occurs in residue 403 out of 410, truncating just the C-terminal 8 amino acids, which is more likely to modulate function than to completely inactivate TrpB, which is essential. Mutant 8 had a



Scheme 5. Synthetic pathway for compounds 40–42.

mutation in *Mb0973c*, which is one of 2 orthologs of chorismate mutase in mycobacteria [24]; a mutation in this gene could also conceivably influence flux through the Trp pathway, since chorismate is a common metabolic intermediate that interconnects the aromatic amino acid (and shikimate) pathways. The resistance mechanism of mutant 1 remains unidentified.

To test the chemical-genetic interaction between **38** and genes in the Trp pathway, we applied CRISPR interference (CRISPRi) [26] on BCG to achieve an inducible repression of the *trp* genes (Fig. 6 A). As indicated in Fig. 6, comparing to the empty vector or the uninduced controls, the knock-down of *trpB* and *trpD* significantly desensitized BCG to compound **38**. Conversely, the repression of *trpE* and *trpC* had little or no effect on BCG's sensitivity to compound **38** inhibition. The alleviation of compound **38**'s toxic effect by the repression of *trp* genes concurs with the hypothesis that fluoro-anthranilates are metabolized into toxic derivatives - a process that depends on enzymes encoded by the *trp* genes. The exact molecular mechanism, however, requires further elucidation.

3. Discussion

A major constraint in reducing TB epidemic is the rise of strains resistant to one or more of clinically approved drugs, which emphasize the need of novel drugs with novel targets. Genetic knockout strains of *Mtb* have established that Trp biosynthesis is essential for the bacterium to survive *in vivo* and cause disease in animal models [2,4,6]. The *in-vivo* effects of inhibition of tryptophan biosynthesis have been partially attributed to restriction of access to Trp inside macrophages through the action of CD4⁺ T-cell-dependent host-expressed indoleamine 2,3-dioxygenase (IDO-1), which converts intracellular tryptophan pools to kynureine [6]. Moreover, Trp levels are decreased in the cerebrospinal fluid of patients with TB meningitis and decline in the plasma of persons progressing from LTBI to active TB [8,9]. Previously, inhibitors of both TrpAB (BRD-4592 [7]) and TrpE (indole-4-carboxamides [23]) have been reported; while the latter showed antitubercular activity in animal models, the former could not be assessed due to poor PK/PD properties.

Targeting the Trp biosynthesis pathway with substrate analogues is challenging as the corresponding compounds are often found toxic to human cells. Herein, we present a class of anthranilate-like compounds endowed with good antimycobacterial activity and low cytotoxicity. We show how replacing the carboxylic moiety with a hydrazide led to a significant

improvement in both activity and cytotoxicity as compared to the parent compound, **6-FABA**. Our preliminary studies corroborates the hypothesis that this new class of compounds target Trp biosynthesis. Compounds **20**, **31** and **38** and **6-FABA** are inactive in the presence of both Trp and the precursors anthranilate and indole. But they retained activity when chorismate is added to the medium (Table 3). Moreover, the evidence of cross-resistance between **6-FABA** and derivative **38** suggested that the two compounds likely have the same mechanism of action (Table 4). In agreement with the previous observations, the whole genome sequencing (WGS) of **38** resistors identified mutations in the Trp pathway genes *TrpE* (P91H), *TrpD* (T108 N), *TrpC* (V92A), *TrpB* (T198 N, E225G, A132V). Furthermore, one of the **38'** mutants mapped to *Mb0973c* (R68P), that it is annotated in literature as chorismate mutase [27] of the shikimate pathway, which is closely connected to the Trp pathway, confirming that hydrazide analogues of **6-FABA** exert their anti-mycobacterial activity by interfering the mycobacterial Trp biosynthesis.

The fact that resistance mutations were distributed over multiple genes in the Trp biosynthetic pathway suggests that they achieve resistance through modulating metabolic flux through the pathway, rather than mitigating the enzyme-specific inhibitory activities of the FABA derivatives. This is sometimes observed with antimetabolite inhibitors that act as contaminants of a pathway to poison downstream processes [28] (including protein synthesis, in the case of tryptophan). Specifically, Islam et al. have previously reported that fluoro-anthranilates [20] inhibit *Mtb* growth by poisoning Trp pools through the production of fluorinated Trp, the latter is presumably incorporated into nascent peptides and cause global protein stresses. Interestingly, we found that moderate repression of *trpB* or *trpD* (but not *trpE* or *trpC*), two critical enzymes of the mycobacterial Trp biosynthesis pathway, alleviated the antimicrobial activity of a tested fluorophenylbenzohydrazides (compound **38**). As there was no exogenous tryptophan added to the media, dampened *de novo* Trp biosynthesis potentially decreased the amount of fluorophenylbenzohydrazides being converted to toxic intermediate, whereas cell growth was temporarily supported by pre-existing tryptophan pools. Nevertheless, as Trp biosynthetic genes are essential for bacterial growth *in vitro* in the absence of exogenous tryptophan sources [2,6], prolonged *trp* gene repression would also disrupt bacterial growth, imposing limitations on the use of growth-based assays to dissect the antimycobacterial mechanism of fluorophenylbenzohydrazides. Future investigations, for instance, through the isotopic tracing of

Table 1

Minimum Inhibitory Concentration against 99% of *Mtb* H37Rv in 7H9/ADC/Tween 80, GastFe, 7H9/ADC/casitone/Tx after 2 weeks and cytotoxicity in Vero cells of compounds **1–42** and **6-FABA**.

Compound	MIC ₉₉ 7H9/ADC/Tw (μM) ^a	MIC ₉₉ GastFe (μM) ^b	MIC ₉₉ 7H9/DPPC/casitone/Tx (μM) ^c	CC ₅₀ Vero cells (μM) ^d
1	>50	>50	>50	n.t. ^e
2	>50	>50	>50	n.t. ^e
3	>50	>50	>50	n.t. ^e
4	>50	>50	>50	n.t. ^e
5	>50	>50	>50	n.t. ^e
6	>50	>50	>50	n.t. ^e
7	>50	>50	>50	n.t. ^e
8	>50	>50	>50	n.t. ^e
9	>50	>50	>50	n.t. ^e
10	>50	>50	>50	n.t. ^e
11	>50	>50	>50	n.t. ^e
12	>50	>50	>50	n.t. ^e
13	>50	>50	>50	n.t. ^e
14	>50	>50	>50	n.t. ^e
15	>50	>50	>50	n.t. ^e
16	>50	>50	>50	n.t. ^e
17	>50	>50	>50	n.t. ^e
18	>50	>50	>50	n.t. ^e
19	9.4	50	9.4	909
20	12.5	1.56	1.56	2027
21	9.4	2.3	1.56	1362
22	12.5	6.25	1.56	1364
23	25	3.125	3.125	792
24	25	6.25	1.56	>1800
25	12.56	3.125	1.56	373
26	50	12.5	6.25	>1800
27	50	6.25	3.125	1040
28	>50	25	6.25	>1800
29	25	12.5	1.56	>1800
30	>50	25	6.25	n.t. ^e
31	5	1.25	0.625	>1800
32	>50	>50	50	n.t. ^e
33	12.5	0.78	1.56	1308
34	45.45	11.36	2.84	1362
35	>50	>50	50	n.t. ^e
36	>50	25	6.25	1304
37	>50	>50	>50	n.t. ^e
38	1.56	2.3	1.3	>1800
39	1.56	1.4	1.4	>1800
40	50	50	50	n.t. ^e
41	50	50	50	n.t. ^e
42	50	50	50	n.t. ^e
6-FABA	5	n.t. ^e	n.t. ^e	74
INH			0.1	n.t. ^e

^a Activity against *Mtb* H37Rv in 7H9/ADC/Tween80 medium after 2 weeks.

^b Activity against *Mtb* H37Rv in GastFe medium after 2 weeks.

^c Activity against *Mtb* H37Rv in 7H9/DPPC/casitone/Tx medium after 2 weeks.

^d cytotoxicity in Vero cells.

^e Not tested.

Table 2

MICs of **20**, **31** and **38** and **6-FABA** against BCG in 7H9/ADC/Tw, in 7H9/ADC/Tw + chorismate 0.1 mM, in 7H9/ADC/Tw + chorismate 0.5 mM, in 7H9/ADC/Tw + sodium anthranilate 0.1 mM, in 7H9/ADC/Tw + indole 0.1 mM, in 7H9/ADC/Tw + Trp 0.1 mM.

Comp	MIC BCG (μM)					
	7H9/ADC/ Tw ^a	7H9/ADC/Tw + 0.1 mM chorismate ^b	BCG MIC 7H9/ADC/Tw+ 0.5 mM chorismate ^c	7H9/ADC/Tw +0.1 mM sodium anthranilate ^d	7H9/ADC/Tw + 0.1 mM indole ^e	7H9/ADC/ Tw + 0.1 mM Trp ^f
20	2.0	8.15	8.15	>50	>50	>50
31	22.9	45.9	45.9	>50	>50	>50
38	3.5	7.1–14.2	14.2	>50	>50	>50
6-FABA	6.4	6.4	6.4	>50	>50	>50

^a Activity against BCG in 7H9/ADC/Tween 80 medium after 1week of treatment.

^b Activity against BCG in 7H9/ADC/Tween 80 medium added with chorismate 0.1 mM after 1week of treatment.

^c Activity against BCG in 7H9/ADC/Tween 80 medium added with chorismate 0.5 mM after 1week of treatment.

^d Activity against BCG in 7H9/ADC/Tween 80 medium added with anthranilate 0.1 mM after 1week of treatment.

^e Activity against BCG in 7H9/ADC/Tween 80 medium added with indole 0.1 mM after 1week of treatment.

^f Activity against BCG in 7H9/ADC/Tween 80 medium added with Trp 0.1 mM after 1week of treatment.

Table 3

6-FABA BCG resistant mutants: colony number on the plate, **6-FABA** concentrations in the medium, **6-FABA** MIC (μM), **38** MIC (μM) against the resistors and the wild type.

Colony n.	6-FABA concentration ^a	6-FABA MIC (μM) ^b	38 MIC (μM) ^c
1	x5 MIC	103	>50
1	x10 MIC	103	>50
1	x20 MIC	>103	>50
2	x20 MIC	>103	>50
Wt	–	6.4	7.10

^a Concentration of **6-FABA** into the medium.

^b Activity of **6-FABA** against *M. bovis* BCG **6-FABA** resistant mutants.

^c Activity of compound **38** against *M. bovis* BCG **6-FABA** resistant mutants.

fluorophenylbenzohydrazide's metabolic trajectory in mycobacteria, are required to establish a finer-scale model of these processes.

4. Experimental procedures

4.1. Chemistry

Reagents and solvents were obtained from commercial sources (Fluka, Sigma-Aldrich, Alfa Aesar). Analytical TLC was performed on Merck silica gel (60F254) precoated plates (0.25 mm). The compounds were visualized under UV light (254 nm) and/or stained with the relevant reagent. Flash column chromatography was performed on silica gel with pore size 60 Å, 230–400 mesh particle size, and 40–63 μm particle size, with the indicated solvents. The yields refer to the purified products, and they were not optimized.

Table 4

Compound **38** BCG resistant mutants: colony number on the plate, **38** concentrations on the plate, **38** MIC (μM), **6-FABA** MIC (μM) against the resistors and the wild type. Genes in the Tryptophan biosynthesis pathway are boldfaced.

Mutant id (n. ^a)	38 selection concentration (μM) ^b	38 MIC (μM) ^c	6-FABA MIC (μM) ^d	Mutations
Wt	–	7.1	6.4	–
1 (1)	x5 MIC	>50	103	–
2 (2)	x5 MIC	56.7	25.8	TrpC : V92A
3 (3)	x5 MIC	>50	51.5–103	TrpE : P91H
4 (4)	x5 MIC	>50	103	TrpB :T198 N, <i>Mb0310</i> :T165A
5 (1)	x10 MIC	>50	51.5	TrpB :+C in aa 403, <i>Galt</i> :Y293 ^f , <i>CtpI</i> :E109A, <i>Mb0199c</i> :E444D
6 (2)	x10 MIC	>50	103	TrpD :T108 N, <i>CtpI</i> :E109A, <i>Mb0199c</i> :E444D
7 (1)	x20 MIC	n.t. ^e	n.t.	TrpB :E225G, <i>Mb0310</i> :T165A
8 (2)	x20 MIC	n.t.	n.t.	<i>Mb0973c</i> :R68P
9 (3)	x20 MIC	n.t.	n.t.	TrpB :A132V, <i>Mb0310</i> :T165A

^a Colony number on the plate.

^b concentration of compound **38** into the medium.

^c Activity of compound **38** against *M. bovis* BCG **38** resistant mutants.

^d Activity of **6-FABA** against *M. bovis* BCG **38** resistant mutants.

^e Not tested.

^f Stop codon.

Table 5

Functional annotations of hypothetical compound **38** resistance genes.

Protein product/gene locus (<i>M. bovis</i> ^a)	Protein product/gene locus (<i>Mtb</i> homolog ^b)	Protein function
Membrane transport		
<i>CtpI</i> / <i>Mb0111c</i>	<i>CtpI</i> / <i>Rv0107c</i>	Cation-transporting ATPase
–/ <i>Mb0199c</i>	–/ <i>Rv0193c</i>	Unknown
–/ <i>Mb0310</i>	–/ <i>Rv0302</i>	Transcriptional regulator
Tryptophan biosynthesis		
–/ <i>Mb0973c</i>	–/ <i>Rv0948c</i>	Chorismate mutase
<i>TrpE</i> / <i>Mb1635</i>	<i>TrpE</i> / <i>Rv1609</i>	Anthranilate synthase, component I.
<i>TrpC</i> / <i>Mb1637</i>	<i>TrpC</i> / <i>Rv1611</i>	Indole-3-glycerol phosphate synthase
<i>TrpB</i> / <i>Mb1638</i>	<i>TrpB</i> / <i>Rv1612</i>	Tryptophan synthase, β subunit
<i>TrpD</i> / <i>Mb2215c</i>	<i>TrpD</i> / <i>Rv2192c</i>	Anthranilate phosphoribosyltransferase

^{a,b} Annotations were retrieved from the Mycobrowser database [25] and curated manually.

All the solid compounds were obtained as amorphous solids, and melting points were not measured. ¹H NMR (400.13 MHz), and ¹³C NMR (100.6 MHz) were recorded with a Bruker Avance 400 spectrometer. Mass spectra data measurements were performed on a VG-Analytical Autospec Q mass spectrometer. Analytical purity was $\geq 95\%$ unless stated otherwise. The purities of the final compounds were checked using a Waters ZQ2000 coupled with LC Waters 2795 and Waters 2996 PDA detector.

General procedure for the synthesis of compounds 1, 2, 6–16 and 18–39. 1-1'- Carbonyl diimidazole **43** (0.97 mmol; 1.5 eq) was added to a solution of 2-amino- 6-fluoro benzoic acid (0.65 mmol; 1.0 eq) in tetrahydrofuran (7 ml) in a round-bottom flask equipped with a stirring bar in dry conditions. The obtained mixture was stirred for 24 h at room temperature and then the appropriate hydroxylamine **45a,b**, amine **46a-k** or hydrazine **47a-t** was added (1.30 mmol; 2.0 eq) and the reaction mixture was stirred at room temperature for 16 h. At the end the mixture was quenched with saturated aqueous sodium bicarbonate and the organic solution was extracted with ethyl acetate, washed with brine and dried over Na₂SO₄.

After filtration and concentration, the crude material was purified by column chromatography on silica gel with a mixture of dichloromethane/ethyl acetate in the opportune volumes to give the expected products **1, 2, 6–16** and **18–37**.

Hydrochloride salts **38** and **39** were prepared by reacting a solution of the hydrazides **20** or **21** (0.08 mmol, 1 eq) in ethanol (0.5 ml) with aqueous HCl 37% added dropwise. The mixture was stirred for 30 min at room temperature and then the white precipitate was separated by filtration and washed with cold ethanol to obtain the desired products.

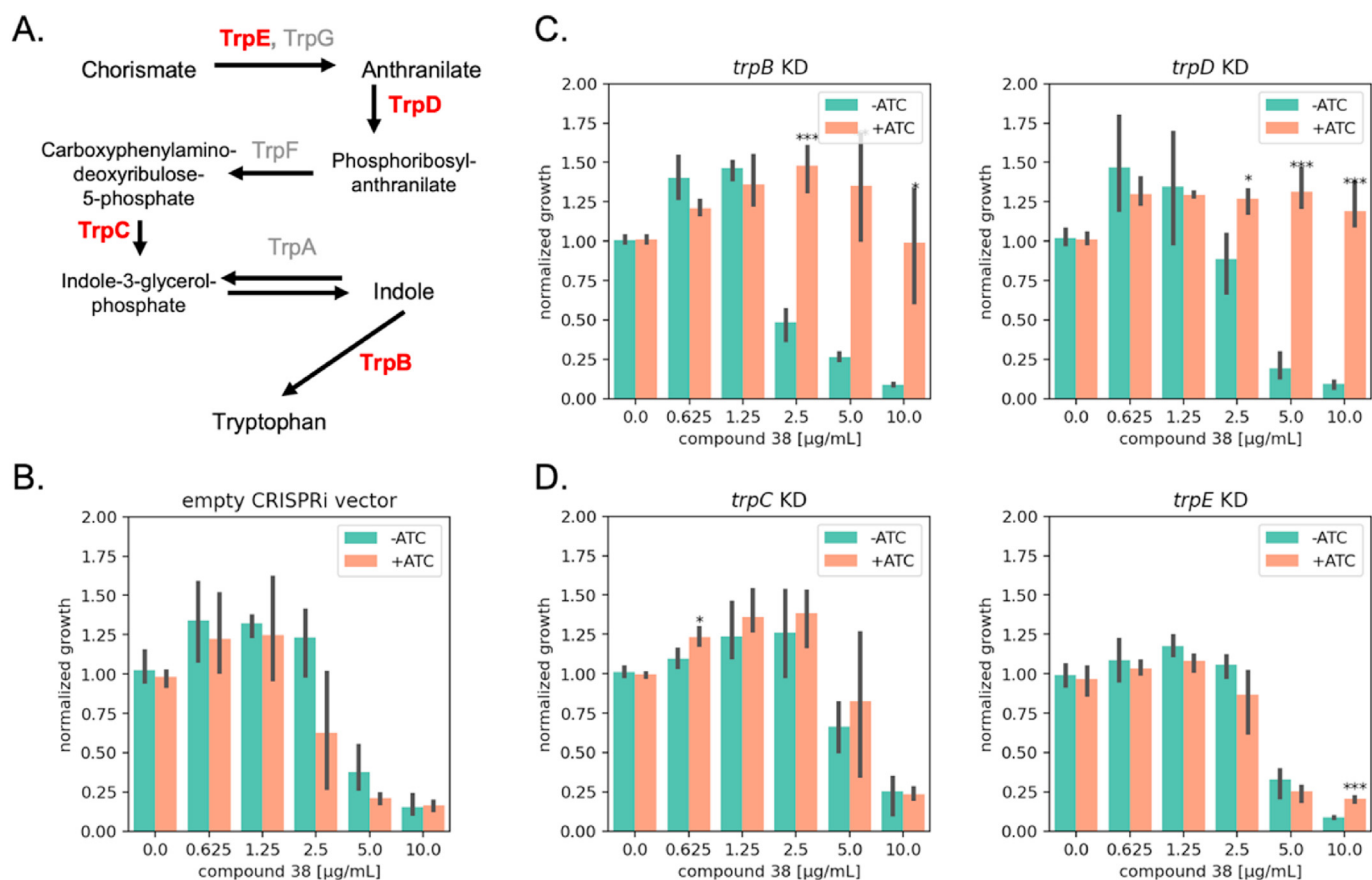


Fig. 6. Transcriptional repression of *trp* genes alleviates compound **38** toxicity. A. Schematic of mycobacterial tryptophan biosynthesis pathway, proteins that are tested in the present study are highlighted by red, bolded text. B–D. Dose-dependent compound **38** inhibition in response to ATC (anhydrotetracycline) induced gene repression. Normalized growth was measured using a resazurin absorbance assay (Supporting information). Error bars represent the standard deviation of data measured from 3 independently isolated colonies (biological triplicate). Statistical significances of growth changes were evaluated using a two-tailed Student's *t*-test, with *, **, and *** denoting *p* values lower than 0.05, 0.01, 0.001, respectively.

2-Amino-6-fluoro-*N*-hydroxybenzamide (1). White solid (26% yield). ^1H NMR (400 MHz, CDCl_3), δ ppm = 7.09 (m, 1H), 6.61 (s broad, 1H), 6.46–6.44 (m, 1H), 6.37–6.32 (m, 1H), 6.06 (s broad, 2H), 5.65 (s broad, 1H). ^{13}C NMR (100 MHz, $\text{DMSO}-d_6$), δ ppm = 166.81, 161.86, 159.43, 149.53, 149.49, 131.88, 131.77, 113.26, 113.24, 107.17, 106.97, 102.08, 101.86. LRMS ($\text{M} + \text{H}^+$) (ESI $^+$) 171.05 [$\text{M} + \text{H}^+$] (calcd for $\text{C}_7\text{H}_8\text{FN}_2\text{O}_2^+$ 171.06).

2-Amino-6-fluoro-*N*-methoxybenzamide (2). White solid (23% yield). ^1H NMR (400 MHz, CDCl_3), δ ppm = 9.19 (d, 1H), 7.18–7.10 (m, 1H), 6.46–6.44 (m, 1H), 6.37–6.32 (m, 1H), 3.90 (s, 3H). ^{13}C NMR (100 MHz, CDCl_3), δ ppm = 166.81, 161.86, 159.43, 149.53, 149.49, 131.88, 131.77, 113.26, 113.24, 107.17, 106.97, 103.92, 103.63, 66.92 LRMS [$\text{M} + \text{H}^+$] (ESI $^+$) (calcd for $\text{C}_8\text{H}_{10}\text{FN}_2\text{O}_2^+$ 185.07).

2-Amino-6-fluorobenzamide (6). White solid (73% yield). ^1H NMR (400 MHz, CDCl_3), δ (ppm): 7.14–7.08 (m, 1H), 6.65 (s broad, 1H), 6.45 (d, 1H, $J = 8.1$ Hz), 6.37–6.31 (m, 1H), 6.12 (s broad, 2H), 5.90 (s broad, 1H). ^{13}C NMR (100 MHz, CDCl_3), δ ppm = 168.30, 163.88, 161.48, 152.23, 152.17, 132.85, 132.72, 113.12, 113.10, 102.92, 102.66, 100.00. LRMS ($\text{M} + \text{H}^+$) (ESI $^+$) 155.08 [$\text{M} + \text{H}^+$] (calcd for $\text{C}_7\text{H}_8\text{FN}_2\text{O}^+$ 155.06).

2-Amino-6-fluoro-*N*'-isopropylbenzamide (7). White-grey solid (67% yield). ^1H NMR (400 MHz, CDCl_3), δ ppm = 7.11–7.03 (m, 1H), 6.45–6.42 (m, 2H), 6.37–6.31 (m, 1H), 4.32–4.19 (m, 1H), 1.25 (d, 6H, $J = 6.6$ Hz). ^{13}C NMR (100 MHz, CDCl_3), δ ppm = 167.66, 163.82, 161.03, 151.52, 132.17, 132.10, 113.07, 103.12, 102.85, 48.38, 22.79. LRMS ($\text{M} + \text{H}^+$) (ESI $^+$) 197.12 [$\text{M} + \text{H}^+$] (calcd for $\text{C}_{10}\text{H}_{14}\text{FN}_2\text{O}^+$ 197.11).

2-Amino-6-fluoro-*N*-(2-hydroxyethyl) benzamide (8). Yellowish oil (15% yield). ^1H NMR (400 MHz, CDCl_3), δ ppm = 7.12–7.07 (m, 2H), 6.46–6.44 (m, 1H), 6.38–6.34 (m, 1H), 5.81 (s broad, 2H), 3.82 (t, 2H, $J = 6.4$ Hz), 3.61 (t, 2H, $J = 6.4$ Hz), 2.66 (s broad, 1H). ^{13}C NMR (100 MHz, CDCl_3) δ ppm = 168.32, 161.57, 159.55, 149.37, 149.31, 134.06, 134.00, 112.28, 112.26, 106.52, 106.36, 105.24, 105.07, 60.61, 44.22. LRMS ($\text{M} + \text{H}^+$) (ESI $^+$) 199.11 [$\text{M} + \text{H}^+$] (calcd for $\text{C}_9\text{H}_{12}\text{FN}_2\text{O}_2^+$ 199.09).

2-Amino-*N*-cyclopropyl-6-fluorobenzamide (9). White solid (25% yield). ^1H NMR (400 MHz, CDCl_3), δ ppm = 7.11–7.03 (m), 6.73 (d, 1H), 6.44 (d, 1H, $J = 8.1$ Hz), 6.35–6.28 (m, 1H), 2.90–2.83 (m, 1H), 0.89–0.82 (m, 2H), 0.62–0.56 (m, 2H). ^{13}C NMR (100 MHz, CDCl_3), δ ppm = 167.66, 163.82, 161.03, 151.52, 132.17, 132.10, 113.07, 103.12, 102.85, 22.79, 6.79. LRMS ($\text{M} + \text{H}^+$) (ESI $^+$) 195.11 [$\text{M} + \text{H}^+$] (calcd for $\text{C}_{10}\text{H}_{12}\text{FN}_2\text{O}^+$ 195.09). ^{13}C NMR (100 MHz, CDCl_3), δ ppm = 167.66, 163.82, 161.03, 151.52, 132.17, 132.10, 113.07, 103.12, 102.85, 22.79, 6.79. LRMS ($\text{M} + \text{H}^+$) (ESI $^+$) 195.11 [$\text{M} + \text{H}^+$] (calcd for $\text{C}_{10}\text{H}_{12}\text{FN}_2\text{O}^+$ 195.09).

2-Amino-*N*-cyclobutyl-6-fluorobenzamide (10). White solid (25% yield). ^1H NMR (400 MHz, CDCl_3), δ ppm = 7.11–7.04 (m, 1H), 6.76 (s broad, 1H), 6.45–6.42 (m, 1H), 6.35–6.28 (m, 1H), 4.61–4.48 (m, 1H), 2.47–2.37 (m, 2H), 2.02–1.89 (m, 2H), 1.83–1.72 (m, 2H). ^{13}C NMR (100 MHz, $\text{DMSO}-d_6$), δ ppm = 163.59, 161.92, 159.35, 149.90, 139.78, 131.26, 131.03, 111.76, 108.86, 108.67, 102.38, 102.23, 50.30, 32.67, 17.96. LRMS ($\text{M} + \text{H}^+$) (ESI $^+$) 209.12 [$\text{M} + \text{H}^+$] (calcd for $\text{C}_{11}\text{H}_{14}\text{FN}_2\text{O}^+$ 209.11).

2-Amino-6-fluorophenyl(pyrrolidin-1-yl)methanone (11). White solid (30% yield). ^1H NMR (400 MHz, CDCl_3), δ ppm = 7.10–7.05 (m, 1H), 6.49–6.40 (m, 2H), 3.66 (t, 2H, $J = 6.9$ Hz), 3.41–3.37 (m, 2H), 2.02–1.84 (m, 4H). ^{13}C NMR (100 MHz, CDCl_3), δ ppm = 168.30, 163.88, 161.48, 152.23, 152.17, 132.85, 132.72, 113.12, 113.10, 102.92, 102.66, 100, 50.30, 22.79. LRMS (M + H) $^+$ (ESI $^+$) 209.12 [M + H] $^+$ (calcd for $\text{C}_{11}\text{H}_{14}\text{FN}_2\text{O}^+$ 209.11).

2-Amino-6-fluorophenyl(4-methylpiperazin-1-yl)methanone (12). White solid (53% yield). ^1H NMR (400 MHz, CDCl_3), δ ppm = 7.11–7.06 (m, 1H), 6.50–6.39 (m, 2H), 4.29 (s broad, 2H), 3.87–3.73 (m, 2H), 3.46–3.34 (m, 2H), 2.57–2.32 (m, 7H). ^{13}C NMR (100 MHz, $\text{DMSO}-d_6$), δ ppm = 164.89, 161.78, 159.46, 148.92, 148.83, 131.26, 131.15, 111.44, 108.86, 108.67, 102.58, 102.29, 54.91, 50.13, 44.96. LRMS (M + H) $^+$ (ESI $^+$) 238.13 [M + H] $^+$ (calcd for $\text{C}_{12}\text{H}_{17}\text{FN}_3\text{O}^+$ 238.14).

2-Amino-N-cyclohexyl-6-fluorobenzamide (13). White solid (70% yield). ^1H NMR (400 MHz, $\text{DMSO}-d_6$), δ ppm = 8.04–8.02 (m, 1H), 7.08–7.03 (m, 1H), 6.50 (d, 1H, $J = 8.1$ Hz), 6.33–6.29 (m, 1H), 5.73 (s broad, 2H), 3.75 (s broad, 1H), 1.82–1.70 (m, 4H), 1.59–1.56 (m, 1H), 1.34–1.11 (m, 5H). ^{13}C NMR (100 MHz, $\text{DMSO}-d_6$), δ ppm = 163.59, 161.92, 159.35, 149.90, 149.78, 131.26, 131.03, 111.76, 108.86, 108.67, 102.38, 102.23, 48.38, 32.67, 25.68, 25.12. LRMS (M + H) $^+$ (ESI $^+$) 237.13 [M + H] $^+$ (calcd for $\text{C}_{13}\text{H}_{18}\text{FN}_2\text{O}^+$ 237.14).

2-Amino-6-fluorophenyl(piperidin-1-yl)methanone (14). Grey solid (42% yield). ^1H NMR (400 MHz, CDCl_3), δ ppm = 7.12–7.04 (m, 1H), 6.50–6.39 (m, 2H), 3.84–3.65 (m, 3H), 3.40–3.27 (m, 3H), 1.63–1.46 (m, 4H). ^{13}C NMR (100 MHz, $\text{DMSO}-d_6$), δ ppm = 164.11, 161.39, 159.10, 149.94, 148.87, 131.22, 131.05, 112.25, 104.47, 103.23, 102.67, 48.50, 24.94, 23.42. LRMS (M + H) $^+$ (ESI $^+$) 222.13 [M + H] $^+$ (calcd for $\text{C}_{12}\text{H}_{15}\text{FN}_2\text{O}^+$ 222.12).

2-Amino-6-fluorophenyl(morpholino)methanone (15). White solid (42% yield). ^1H NMR (400 MHz, CDCl_3), δ ppm = 7.12–7.07 (m, 1H), 6.51–6.40 (m, 2H), 3.90–3.69 (m, 5H), 3.64–3.57 (m, 1H), 3.51–3.44 (m, 1H), 3.36–3.33 (m, 1H). ^{13}C NMR (100 MHz, CDCl_3), δ ppm = 168.30, 163.88, 161.43, 152.23, 152.17, 132.85, 132.72, 113.12, 113.10, 102.92, 102.66, 100, 66.62, 45.56. LRMS (M + H) $^+$ (ESI $^+$) 225.09 [M + H] $^+$ (calcd for $\text{C}_{11}\text{H}_{14}\text{FN}_2\text{O}_2$ + 225.10).

2-Amino-6-fluoro-N-(4-fluorophenyl) benzamide (16). White solid (12% yield). ^1H NMR (400 MHz, CDCl_3), δ ppm = 8.33–8.29 (d, 1H), 7.55–7.53 (m, 2H), 7.19–7.15 (m, 1H), 7.13–7.04 (m, 2H), 6.55–6.53 (d, 1H, $J = 8.1$ Hz), 6.47–6.41 (m, 1H). ^{13}C NMR (100 MHz, CDCl_3), δ ppm = 168.30, 150.24, 150.18, 146.22, 132.15, 132.04, 115.76, 115.54, 114.01, 111.93, 102.71. LRMS (M + H) $^+$ (ESI $^+$) 248.09 [M + H] $^+$ (calcd for $\text{C}_{13}\text{H}_{11}\text{F}_2\text{N}_2\text{O}^+$ + 248.08).

tert-butyl 2-(2-amino-6-fluorobenzoyl)hydrazine-1-carboxylate (18). White solid (60% yield). ^1H NMR (400 MHz, CDCl_3), δ ppm = 8.32 (d, 1H), 7.16–7.11 (m, 1H), 6.66 (s broad, 1H), 6.48 (d, 1H, $J = 8.1$ Hz), 6.38–6.35 (m, 1H), 1.50 (s, 9H). ^{13}C NMR (100 MHz, $\text{DMSO}-d_6$), δ ppm = 164.69, 159.61, 155.89, 149.41, 131.88, 131.77, 111.43, 102.08, 101.86, 80.03, 28.56. LRMS (M + H) $^+$ (ESI $^+$) 270.10 [M + H] $^+$ (calcd for $\text{C}_{12}\text{H}_{17}\text{FN}_3\text{O}_3$ 270.12).

2-Amino-N'-cyclohexyl-6-fluorobenzohydrazide (19). White solid (33% yield). ^1H NMR (400 MHz, CDCl_3), δ ppm = 7.12–7.08 (m, 1H), 6.45 (d, 1H, $J = 8.1$ Hz), 6.38–6.33 (m, 1H), 2.90–2.85 (m, 1H), 1.94–1.18 (m, 11H). ^{13}C NMR (100 MHz, $\text{DMSO}-d_6$), δ ppm = 168.30, 161.92, 159.35, 149.90, 149.78, 131.26, 131.03, 111.76, 108.86, 108.67, 102.38, 102.23, 48.38, 32.67, 25.68, 25.12. LRMS (M + H) $^+$ (ESI $^+$) 252.17 [M + H] $^+$ (calcd for $\text{C}_{13}\text{H}_{19}\text{FN}_3\text{O}^+$ 252.15).

2-Amino-6-fluoro-N'-phenylbenzohydrazide (20). White solid (yield 25%). ^1H NMR (400 MHz, CDCl_3), δ ppm = 8.36 (d, 1H), 7.28–7.24 (m, 2H), 7.18–7.12 (m, 1H), 6.95–6.91 (m, 3H), 6.48–6.38 (m, 2H), 6.07 (s broad, 2H). ^{13}C NMR (100 MHz, CDCl_3), δ ppm = 170.02, 159.82, 153.02, 148.78, 133.21, 128.85, 119.39,

115.62, 113.12, 106.58, 100.78. LRMS (M + H) $^+$ (ESI $^+$) 246.11 [M + H] $^+$ (calcd for $\text{C}_{13}\text{H}_{13}\text{FN}_3\text{O}^+$ + 246.10).

2-Amino-6-fluoro-N'-(4-fluorophenyl) benzohydrazide (21). White solid (17% yield). ^1H NMR (400 MHz, CDCl_3), δ ppm = 8.36 (d, 1H), 7.18–7.13 (m, 1H), 6.89–6.81 (m, 4H), 6.48–6.38 (m, 2H), 5.92 (s broad, 2H). ^{13}C NMR (100 MHz, CDCl_3), δ ppm = 165.05, 150.25, 150.18, 146.22, 132.15, 132.04, 115.76, 115.54, 114.01, 111.93, 102.71, 102.38. LRMS (M + H) $^+$ (ESI $^+$) 264.06 [M + H] $^+$ (calcd for $\text{C}_{13}\text{H}_{12}\text{F}_2\text{N}_3\text{O}^+$ 264.09).

2-Amino-6-fluoro-N'-(3-fluorophenyl) benzohydrazide (22). White solid (17% yield). ^1H NMR (400 MHz, $\text{DMSO}-d_6$), δ ppm = 10.10 (s broad, 1H), 8.23 (s broad, 1H), 7.21–7.12 (m, 2H), 6.64–6.61 (m, 1H), 6.57–6.48 (m, 3H), 6.43–6.38 (m, 1H), 5.80 (s broad, 2H). ^{13}C NMR (100 MHz, CDCl_3), δ ppm = 166.91, 161.86, 161.73, 161.15, 152.12, 148.34, 148.28, 147.94, 147.99, 133.44, 133.14, 133.11, 130.75, 115.28, 113.35, 113.33, 113.22, 107.10, 106.94, 103.14, 102.88, 101.34, 101.18. LRMS (M + H) $^+$ (ESI $^+$) 264.10 [M + H] $^+$ (calcd for $\text{C}_{13}\text{H}_{12}\text{F}_2\text{N}_3\text{O}^+$ 264.09).

2-Amino-N'-(2-chlorophenyl)-6-fluorobenzohydrazide (23). Brownish solid (yield 18%). ^1H NMR (400 MHz, CDCl_3), δ ppm = 8.36 (d, 1H), 7.31 (dd, 1H, $J = 8.1$ Hz, 1.7 Hz), 7.19–7.14 (m, 2H), 7.01 (dd, 1H, $J = 8.1$ Hz, 1.7 Hz), 6.85 (td, 1H, $J = 8.1$ Hz, 1.7 Hz), 6.49–6.39 (m, 2H). ^{13}C NMR (100 MHz, CDCl_3), δ ppm = 166.56, 161.19, 152.13, 152.06, 144.08, 133.33, 133.12, 129.48, 127.76, 121.48, 119.62, 113.80, 113.26, 113.24, 103.07, 102.81. LRMS (M + H) $^+$ (ESI $^+$) 280.08 [M + H] $^+$ (calcd for $\text{C}_{13}\text{H}_{12}\text{ClFN}_3\text{O}^+$ + 280.06).

2-Amino-N'-(3-chlorophenyl)-6-fluorobenzohydrazide (24). White solid (yield 35%). ^1H NMR (400 MHz, CDCl_3), δ ppm = 8.35 (d, 1H), 7.19–7.14 (m, 2H), 6.92 (t, 1H, $J = 1.5$ Hz), 6.89–6.88 (m, 1H), 6.82 (dd, 1H, $J = 8.1$ Hz, 1.5 Hz), 6.48 (d, 1H, $J = 8.1$ Hz), 6.44–6.39 (m, 2H). ^{13}C NMR (100 MHz, CDCl_3), δ ppm = 166.56, 161.19, 149.47, 149.40, 144.08, 134.11, 134.05, 133.28, 129.48, 127.76, 121.48, 113.80, 113.26, 112.26, 112.23, 103.07, 102.81. LRMS (M + H) $^+$ (ESI $^+$) 280.07 [M + H] $^+$ (calcd for $\text{C}_{13}\text{H}_{12}\text{ClFN}_3\text{O}^+$ + 280.06).

2-Amino-N'-(4-chlorophenyl)-6-fluorobenzohydrazide (25). Yellowish solid (yield 70%). ^1H NMR (400 MHz, CDCl_3), δ ppm = 8.35 (d, 1H), 7.20–7.13 (m, 3H), 6.88 (d, 2H, $J = 8.8$ Hz), 6.46–6.38 (m, 2H), 6.26 (s broad, 1H), 5.95 (s broad, 2H). ^{13}C NMR (100 MHz, CDCl_3), δ ppm = 166.84, 163.59, 161.16, 152.06, 151.99, 146.92, 133.26, 133.13, 129.21, 126.10, 114.92, 113.26, 113.24, 103.12, 102.86. LRMS (M + H) $^+$ (ESI $^+$) 280.04 [M + H] $^+$ (calcd for $\text{C}_{13}\text{H}_{12}\text{ClFN}_3\text{O}^+$ + 280.06).

2-Amino-N'-(2,3-dichlorophenyl)-6-fluorobenzohydrazide (26). Yellowish solid (yield 13%). ^1H NMR (400 MHz, CDCl_3), δ ppm = 8.38 (d, 1H), 7.20–7.14 (m, 1H), 7.11 (t, 1H, $J = 8.1$ Hz), 7.01 (dd, 1H, $J = 8.1$ Hz, 1.4 Hz), 6.91 (dd, 1H, $J = 8.1$ Hz, 1.4 Hz), 6.72 (s broad, 1H), 6.50–6.40 (m, 2H). ^{13}C NMR (100 MHz, CDCl_3), δ ppm = 166.91, 161.15, 150.14, 149.91, 146.28, 133.44, 133.31, 130.75, 127.47, 119.29, 116.08, 112.57, 11.75, 103.14, 102.88. LRMS (M + H) $^+$ (ESI $^+$) 314.05 [M + H] $^+$ (calcd for $\text{C}_{13}\text{H}_{11}\text{Cl}_2\text{FN}_3\text{O}^+$ 314.03).

2-Amino-N'-(2,4-dichlorophenyl)-6-fluorobenzohydrazide (27). Grey solid (yield 28%); ^1H NMR (400 MHz, CDCl_3), δ ppm = 8.36 (d, 1H), 7.33 (d, 1H, $J = 2.2$ Hz), 7.15–7.12 (m, 2H), 6.92 (d, 1H, $J = 8.3$ Hz), 6.59 (s broad, 1H), 6.49–6.39 (m, 2H). ^{13}C NMR (100 MHz, CDCl_3), δ ppm = 166.91, 161.15, 150.14, 149.91, 142.85, 133.44, 133.31, 128.60, 127.74, 126.97, 119.29, 116.08, 112.57, 111.75, 103.14, 102.88. LRMS (M + H) $^+$ (ESI $^+$) 314.06 [M + H] $^+$ (calcd for $\text{C}_{13}\text{H}_{11}\text{Cl}_2\text{FN}_3\text{O}^+$ 314.03).

2-Amino-N'-(2,5-dichlorophenyl)-6-fluorobenzohydrazide (28). Yellowish solid (yield 29%). ^1H NMR (400 MHz, $\text{DMSO}-d_6$), δ ppm = 10.26 (s broad, 1H), 7.90 (s broad, 1H), 7.35 (d, 1H, $J = 8.2$ Hz), 7.17–7.11 (m, 1H), 6.82–6.79 (m, 2H), 6.55–6.53 (m, 1H), 6.42–6.38 (m, 1H), 5.80 (s broad, 2H). ^{13}C NMR (100 MHz, $\text{DMSO}-d_6$), δ ppm = 181.84, 164.99, 150.14, 149.91, 146.28, 133.03, 132.11, 132.07, 131.03, 119.29, 116.08, 112.57, 111.75, 102.22, 102.07.

LRMS (M + H)⁺(ESI⁺) 314.04 [M + H]⁺(calcd for C₁₃H₁₁Cl₂FN₃O⁺ 314.03).

2-Amino-N'-(3,4-dichlorophenyl)-6-fluorobenzohydrazide (29). White solid (yield 18%). ¹H NMR (400 MHz, CDCl₃), δ ppm = 8.36 (d, 1H), 7.26 (d, 1H, *J* = 8.7 Hz), 7.20–7.14 (m, 1H), 7.02 (d, 1H, *J* = 2.6 Hz), 6.78 (dd, 1H, *J* = 8.7, 2.6 Hz), 6.49–6.29 (m, 2H). ¹³C NMR (100 MHz, CDCl₃), δ ppm = 166.91, 161.15, 152.12, 147.94, 147.89, 133.44, 133.31, 133.11, 130.75, 124.03, 115.28, 113.35, 113.33, 113.22, 103.14, 102.88. LRMS (M + H)⁺(ESI⁺) 314.05 [M + H]⁺(calcd for C₁₃H₁₁Cl₂FN₃O⁺ 314.03).

2-Amino-N'-(3,5-dichlorophenyl)-6-fluorobenzohydrazide (30). Yellowish solid (yield 20%). ¹H NMR (400 MHz, DMSO-*d*₆), δ ppm = 6.38–6.32 (m, 1H), 6.01–5.99 (m, 3H), 5.76 (m, 1H), 5.63–5.58 (m, 1H). ¹³C NMR (100 MHz, DMSO-*d*₆), δ ppm = 164.99, 161.73, 159.71, 150.14, 149.91, 146.28, 132.11, 132.07, 131.03, 121.56, 116.08, 112.57, 111.75, 102.22, 102.07. LRMS (M + H)⁺(ESI⁺) 314.03 [M + H]⁺(calcd for C₁₃H₁₁Cl₂FN₃O⁺ 314.03).

2-Amino-6-fluoro-N'-(2,4,6-trichlorophenyl) benzohydrazide (31). White solid (yield 63%). ¹H NMR (400 MHz, DMSO-*d*₆), δ ppm = 10.27 (s broad, 1H), 7.53 (s broad, 3H), 7.11–7.05 (m, 1H), 6.49–6.47 (m, 1H), 6.30–6.28 (m, 1H), 5.84 (s broad, 2H). ¹³C NMR (100 MHz, DMSO-*d*₆), δ ppm = 166.56, 161.19, 149.47, 149.40, 140.99, 133.33, 133.12, 127.76, 125.36, 125.30, 113.60, 113.26, 103.07, 102.81. LRMS (M + H)⁺(ESI⁺) 347.98 [M + H]⁺(calcd for C₁₃H₁₀Cl₃FN₃O⁺ 347.99).

2-Amino-N'-benzyl-6-fluorobenzohydrazide (32). White solid (yield 35%). ¹H NMR (400 MHz, CDCl₃), δ ppm = 8.03 (s broad, 1H), 7.42–7.30 (m, 5H), 7.10–7.07 (m, 1H), 6.46–6.44 (m, 1H), 6.35–6.29 (m, 1H), 5.81 (s broad, 2H), 4.07 (s, 2H). ¹³C NMR (100 MHz, CDCl₃), δ ppm = 166.84, 163.59, 161.16, 152.06, 151.99, 146.92, 133.26, 133.13, 129.21, 126.10, 114.92, 113.26, 113.24, 103.12, 102.86, 53.87. LRMS (M + H)⁺(ESI⁺) 260.14 [M + H]⁺(calcd for C₁₄H₁₅FN₃O⁺ 260.12).

2-Amino-6-fluoro-N'-(4-methoxyphenyl) benzohydrazide (33). White solid (yield 35%); ¹H NMR (400 MHz, CDCl₃), δ ppm = 8.44 (s broad, 1H), 7.17–7.12 (m, 1H), 6.91 (d, 2H, *J* = 8.8 Hz), 6.82 (d, 2H, *J* = 8.8 Hz), 6.54–6.52 (m, 1H), 6.47–6.42 (m, 1H), 3.75 (s, 3H). ¹³C NMR (100 MHz, CDCl₃), δ ppm = 166.284, 163.59, 161.16, 153.70, 152.06, 151.99, 141.42, 141.37, 133.26, 133.13, 116.70, 114.92, 113.26, 113.24, 103.12, 102.86, 55.30. LRMS (M + H)⁺(ESI⁺) 276.14 [M + H]⁺(calcd for C₁₄H₁₅FN₃O₂⁺ 276.11).

2-Amino-6-fluoro-N'-(4-(trifluoromethyl) phenyl) benzohydrazide (34). Yellowish solid (yield 18%). ¹H NMR (400 MHz, CDCl₃), δ ppm = 8.38 (d, 1H), 7.50 (d, 2H, *J* = 8.5 Hz), 7.20–7.15 (m, 1H), 6.97 (d, 2H, *J* = 8.5 Hz), 6.49–6.40 (m, 2H), 5.95 (s broad, 1H). ¹³C NMR (100 MHz, CDCl₃), δ ppm = 161.73, 159.71, 149.47, 149.40, 147.90, 134.11, 134.05, 127.10, 125.51, 125.47, 125.44, 125.41, 124.96, 124.80, 124.55, 124.29, 124.04, 122.82, 120.67, 115.91, 115.90, 115.89, 115.87, 112.26, 112.23, 105.58, 105.42, 105.03, 104.87. LRMS (M + H)⁺(ESI⁺) 314.05 [M + H]⁺(calcd for C₁₄H₁₂F₄N₃O⁺ 314.09).

2-Amino-6-fluoro-N'-(2-nitrophenyl) benzohydrazide (35). Yellow solid (yield 30%). ¹H NMR (400 MHz, DMSO-*d*₆), δ ppm = 10.56 (s broad, 1H), 9.49 (s broad, 1H), 8.13 (d, 1H, *J* = 8.1 Hz), 7.64 (t, 1H, *J* = 8.1 Hz), 7.19–7.11 (m, 2H), 6.87 (t, 1H, *J* = 8.1 Hz), 6.54 (d, 1H, *J* = 8.1 Hz), 6.41–6.36 (m, 1H), 5.91 (s broad, 2H). ¹³C NMR (100 MHz, DMSO-*d*₆), δ ppm = 170.95, 162.23, 159.83, 149.84, 149.78, 145.74, 136.85, 132.11, 131.87, 126.34, 118.33, 115.10, 111.72, 106.75, 106.65, 102.00, 101.78. LRMS (M + H)⁺(ESI⁺) 291.06 [M + H]⁺(calcd for C₁₃H₁₂FN₄O₃⁺ 291.09).

2-Amino-6-fluoro-N'-(3-nitrophenyl) benzohydrazide (36). Yellow solid (yield 25%). ¹H NMR (400 MHz, DMSO-*d*₆), δ ppm = 10.24 (s broad, 1H), 8.59 (s broad, 1H), 7.59–7.56 (m, 2H), 7.45 (t, 1H, *J* = 8.1 Hz), 7.21–7.13 (m, 2H), 6.57 (d, 1H, *J* = 8.1 Hz), 6.45–6.40 (m, 1H), 5.82 (s broad, 2H). ¹³C NMR (100 MHz, 400 MHz, DMSO-*d*₆), δ ppm = 165.19, 162.27, 159.80, 150.97, 150.43,

150.37, 149.19, 132.40, 132.29, 130.61, 118.96, 113.39, 112, 106.14, 105.78, 102.53, 102.31. LRMS (M + H)⁺(ESI⁺) 291.10 [M + H]⁺(calcd for C₁₃H₁₂FN₄O₃⁺ 291.09).

2-Amino-N'-(2,4-dinitrophenyl)-6-fluorobenzohydrazide (37). Orange solid (yield 15%), ¹H NMR (400 MHz, DMSO-*d*₆), δ ppm = 10.34 (s broad, 1H), 8.91 (d, 1H, *J* = 2.5 Hz), 8.43 (dd, *J* = 9.5, 2.5 Hz), 7.26 (d, 1H, *J* = 9.5 Hz), 7.19–7.13 (m, 1H), 6.55 (d, 1H, *J* = 8.1 Hz), 6.42–6.38 (m, 1H). ¹³C NMR (100 MHz, DMSO-*d*₆), δ ppm = 165.77, 162.23, 159.83, 149.84, 149.78, 145.74, 136.85, 136.44, 134.11, 134.05, 131.80, 128.91, 122.81, 115.10, 111.72, 106.75, 106.65, 102, 101.78. LRMS (M + H)⁺(ESI⁺) 336.10 [M + H]⁺(calcd for C₁₃H₁₁FN₅O₅⁺ 336.07).

2-Amino-6-fluoro-N'-phenylbenzohydrazide hydrochloride (38). White solid 90% yield ¹H NMR (400 MHz, DMSO-*d*₆), δ ppm = 10.04 (s broad, 1H), 7.18–7.12 (m, 1H), 7.03–6.99 (m, 2H), 6.81–6.79 (m, 2H), 6.73–6.70 (m, 1H), 6.59 (d, 1H, *J* = 8.1 Hz), 6.45–6.41 (m, 1H). ¹³C NMR (100 MHz, DMSO-*d*₆), δ ppm = 166.12, 166.06, 160.40, 158.39, 146.21, 141.46, 141.40, 132.19, 132.13, 128.68, 121.35, 117.06, 117.04, 116.05, 115.89, 115.08, 109.95, 109.79.

2-Amino-6-fluoro-N'-(4-fluorophenyl) benzohydrazide hydrochloride (39). White solid 90% yield. ¹H NMR (400 MHz, DMSO-*d*₆), δ ppm = 10.07 (s broad, 1H), 7.18–7.12 (m, 1H), 7.03–6.99 (m, 2H), 6.81–6.78 (m, 2H), 6.59 (d, 1H, *J* = 8.1 Hz), 6.45–6.41 (m, 1H). ¹³C NMR (400 MHz, DMSO-*d*₆), δ ppm = 166.12, 166.06, 160.40, 158.67, 158.39, 156.66, 143.53, 143.51, 141.46, 141.40, 132.19, 132.13, 117.10, 117.06, 117.03, 116.05, 115.89, 114.94, 114.78, 109.95, 109.79.

Preparation of (Z)-2-amino-6-fluoro-N'-hydroxybenzimidamide (50). Hydroxylamine hydrochloride (1.53 mmol; 2.1 eq) and potassium hydroxide (2.2 mmol; 3.0 eq) were added to a solution of 2-amino-6-fluorobenzonitrile **48** (0.73 mmol; 1.0 eq) in dry methanol (1 ml) at room temperature, and the reaction mixture was stirred for 24 h at room temperature. At the end the reaction mixture was concentrated, dissolved in water and extracted with ethyl acetate. Then the organic layer was washed with brine, dried over Na₂SO₄ and concentrated *in vacuo*. The crude material was purified by column chromatography on silica gel and a mixture of dichloromethane/ethyl acetate (10:1, v/v), and crystallized with diethyl ether to give **50** as a brownish powder.

Preparation of 3-fluoro-2-(5-methyl-1,2,4-oxadiazol-3-yl) aniline (3). Potassium *tert*-butoxide (0.57 mmol; 1.9 eq) and *tert*-butyl acetate (15 ml) were added to a solution of **50** (0.3 mmol; 1.0 eq) in 5 ml of dry *tert*-butanol. The reaction mixture was heated to reflux and stirred for 2.5 h. At the end, the reaction mixture was concentrated *under vacuum*, and the residue was diluted with water, extracted with ethyl acetate and dried over Na₂SO₄. The crude material obtained after filtration and solvent evaporation was purified by column chromatography on silica gel and a mixture of cyclohexane/ethyl acetate (6:1, v/v) to give the desired product **3** as a white powder (55% yield); ¹H NMR (400 MHz, DMSO-*d*₆), δ ppm = 7.22–7.17 (m, 1H), 6.64 (d, 1H, *J* = 8.1 Hz), 6.41 (m, 1H), 6.25 (s broad, 2H), 2.68 (s, 3H). ¹³C NMR (DMSO-*d*₆), δ ppm = 176.74, 176.73, 164.24, 164.21, 163.08, 160.60, 150.16, 150.11, 132.73, 132.61, 111.99, 111.96, 102.49, 102.27, 98.03, 97.87, 12.42.

Preparation of 3-fluoro-2-(hydrazinyl)benzenammonium trifluoroacetate salt (17). Trifluoroacetic acid (5 ml) was added to a solution of **18** (0.07 mmol, 1 eq) in dry DCM (5 ml) and the reaction mixture was stirred for 30 min at room temperature. Then the solvent was evaporated and the final product **17** was precipitated as white powder (>90% yield); White solid (>90% yield). ¹H NMR (400 MHz, DMSO-*d*₆), δ ppm = 7.20–7.14 (m, 1H), 6.57 (d, 1H, *J* = 8.1 Hz), 6.39–6.35 (m, 1H). ¹³C NMR (100 MHz, CDCl₃), δ ppm = 164.38, 162.32, 159.88, 150.90, 150.84, 133.14, 133.03, 112.27, 112.25, 103.66, 103.48, 102.12, 101.89.

Preparation of 3-fluoro-2-(5-methyl-1,3,4-oxadiazol-2-yl) aniline (4). Triethyl orthoacetate (0,3 mmol; 1,0 eq) was added to a solution of **17** (0,3 mmol; 1,0 eq) in dioxane (2 ml). The reaction mixture was heated to reflux for 24 h, then diluted with water and extracted with dichloromethane. The organic layer was washed with brine, dried over Na_2SO_4 and concentrated to give the crude material, which was then purified by column chromatography on silica gel and a mixture of cyclohexane/ethyl acetate (10:1, v/v) to achieve the desired product **4** as a white powder (24% yield); ^1H NMR (400 MHz, $\text{DMSO}-d_6$), δ ppm = 7.26–7.20 (m, 1H), 6.98 (s broad, 2H), 6.72 (d, 1H, $J = 8.1$ Hz), 6.48–6.43 (m, 1H), 2.58 (s, 3H). ^{13}C NMR (100 MHz, $\text{DMSO}-d_6$), δ ppm = 163.14, 163.13, 162.19, 161.63, 161.60, 159.70, 150.11, 150.06, 133.22, 133.10, 112.07, 112.04, 102.08, 101.87, 94.50, 94.35, 10.96. LRMS ($\text{M} + \text{H}$) $^+$ (ESI $^+$) 194.06 [$\text{M} + \text{H}$] $^+$ (calcd for $\text{C}_9\text{H}_9\text{FN}_3\text{O}^+$ 194.07).

Preparation of 3-fluoro-2-(1H-tetrazol-5-yl) aniline (5). To a solution of 2-amino-6-fluorobenzonitrile **53** (0,73 mmol; 1,0 eq) in 1 ml of dry dimethylformamide, ammonium chloride (4,8 mmol; 13 eq) and sodium azide (4,8 mmol, 13 eq) were added and the reaction mixture was heated to reflux for 24 h. After solvent evaporation, water was added, and the brownish precipitate was filtered off. The liquid layer was extract with ethyl acetate, washed with a solution of 2 N HCl and brine and dried over Na_2SO_4 . After filtration and evaporation, the residue was purified by column chromatography on silica gel and a mixture of dichloromethane/methanol 1% (v/v), to obtain the final product **5** as a white powder (24% yield); ^1H NMR (400 MHz, $\text{DMSO}-d_6$), δ ppm = 7.26–7.22 (m, 1H), 6.72 (d, 1H, $J = 8.1$ Hz), 6.54–6.49 (m, 1H). ^{13}C NMR (100 MHz, $\text{DMSO}-d_6$), δ ppm = 164.24, 164.21, 162.19, 1261.63, 161.60, 159.70, 150.11, 150.06, 133.22, 133.10, 112.07, 112.04, 102.08, 101.87. LRMS ($\text{M} + \text{H}$) $^+$ (ESI $^+$) 194.12 [$\text{M} + \text{H}$] $^+$ (calcd for $\text{C}_7\text{H}_7\text{FN}_5$ 180.07).

Preparation of (2-fluoro-6-nitrophenyl) methanol (55). Water (1.24 ml) and CaCO_3 (2.215 mmol, 5.15 eq) were added to a solution of 2-(bromomethyl)-1-fluoro-3-nitrobenzene (0.43 mmol, 1 eq) in dioxane (1.24 ml), the reaction mixture was refluxed for 8 h. The solution was cooled down to rt and dioxane was removed under reduced pressure. The solid residue was diluted in DCM and dissolved with 1 N HCl at 0 °C. The mixture was extracted with DCM and washed with NaHCO_3 aqueous solution and brine, dried over Na_2SO_4 and filtered off. After solvent evaporation, the crude material was purified by column chromatography on silica gel and a mixture of petroleum ether/ethyl acetate (10:1) to give the **55** as a white powder.

Preparation of 2-fluoro-6-nitrobenzaldehyde (56). To a solution of **55** (1.6 mmol, 1 eq) in anhydrous DCM (10 ml), the Dess-Martin reagent periodinane (2.5 mmol, 1.5 eq) was added at 0 °C. The reaction was stirred for 1 h at room temperature and then quenched with aqueous Na_2HCO_3 and solid $\text{Na}_2\text{S}_2\text{O}_3$. The mixture was extracted with DCM, washed with brine and dried over anhydrous Na_2SO_4 . After filtration and concentration *under vacuum* the yellowish solid residue was purified by column chromatography on silica gel and a mixture of petroleum ether/ethyl acetate (10:1) to give **56** as a white solid.

Preparation of 2,2,2-trifluoro-1-(2-fluoro-6-nitrophenyl) ethan-1-ol (57). To a solution of **56** (0.42 mmol, 1 eq) in anhydrous tetrahydrofuran (1 ml), trifluoromethyltrimethyl silane (0.2 mmol, 2 M in THF, 1.2 eq) and TBAF (1.0 M in THF, 3 μl) were added at 0 °C and stirred. After 15 min, methanol (3 ml) and 2 M HCl (1 ml) were added and the whole mixture was stirred for additional 15 min. Then the solvent was removed under reduced pressure and the aqueous mixture was extracted with dichloromethane, washed with brine and dried over Na_2SO_4 . The filtered organic layer was concentrated *in vacuo* and the final residue was purified by column chromatography on silica gel and a mixture of petroleum ether/ethyl acetate (15:1) to achieve **57** as a brownish oil.

Preparation of 2,2,2-trifluoro-1-(2-fluoro-6-nitrophenyl) ethyl trifluoro methane sulfonate (58). **57** (1.13 mmol, 1 eq) and 2,6-lutidine (1.36 mmol, 1.2 eq) were dissolved in anhydrous DCM (5 ml). The resulting solution was cooled in an ice bath, and trifluoromethanesulfonic anhydride (2.83 mmol, 2.5 eq) was added portion wise. The reaction mixture was stirred at 0–4 °C for 2 h and then quenched by addition of water. The mixture was extracted with dichloromethane, the combined organic layers were washed with brine and dried over Na_2SO_4 and filtered off. The filtrate was concentrated *in vacuo* to give the crude material, which was purified by column chromatography on silica gel and a mixture of petroleum ether/ethyl acetate (15:1) to afford **58** as a brown oil.

General procedure for the preparation of N-substituted 2,2,2-trifluoro-1-(2-fluoro-6-nitrophenyl)ethan-1-amines 59a-c. To a solution of **58** (0.95 mmol, 1 eq) in anhydrous DCM, potassium carbonate (1.85 mmol, 1.95 eq) and the appropriate amine were added (1.55 mmol, 1.63 eq). The mixture was stirred at 75 °C for 16 h then cooled down to room temperature, diluted with 2 N HCl, extracted with dichloromethane and washed with brine. The organic layer was dried over Na_2SO_4 , filtered off and concentrated *in vacuo*. The brownish liquid residue was purified by column chromatography on silica gel and a mixture of petroleum ether/ethyl acetate (15:1) to afford compounds **59a-c**.

General procedure for the preparation of N-substituted 2-(1-amino-2,2,2-trifluoroethyl)-3-fluoroanilines 40–42. To a solution of **59a-c** (0.28 mmol, 1 eq) in acetonitrile/water (1: 0.1 ml) $\text{NiCl}_2 \cdot 6\text{H}_2\text{O}$ (0.056 mmol, 0.2 eq) was added and the mixture was then stirred for 5 min. Afterwards, sodium borohydride (1.4 mmol, 5 eq) as a fine powder was added to the reaction mixture at 0 °C and a black solid immediately precipitated. The reaction mixture was stirred for 30 min and then quenched by addition of water. The mixture was extracted with dichloromethane and the organic layer was dried over Na_2SO_4 . Filtration and evaporation of the solvent gave the crude material that was purified by column chromatography on silica gel with the opportune mixture of cyclohexane/ethyl acetate to afford final compounds **40–42**.

3-Fluoro-2-(2,2,2-trifluoro-1-morpholinoethyl) aniline (40). White solid (64% yield). ^1H NMR (400 MHz, CDCl_3), δ ppm = 7.07–7.02 (m, 1H), 6.43–6.35 (m, 2H), 4.93 (s broad, 2H), 4.36 (q, 1H, $J = 8.3$ Hz), 3.79–3.70 (m, 4 H), 2.67 (s broad, 2H), 2.61–2.56 (m, 2H). ^{13}C NMR (100 MHz, CDCl_3), δ ppm = 161.98, 161.27, 148.20, 148.16, 130.73, 130.62, 119.79, 119.67, 111.78, 103.92, 103.63, 66.92, 63.86, 63.74, 51.98. LRMS ($\text{M} + \text{H}$) $^+$ (ESI $^+$) 279.08 [$\text{M} + \text{H}$] $^+$ (calcd for $\text{C}_{12}\text{H}_{15}\text{F}_4\text{N}_4\text{O}_2^+$ 279.11).

3-Fluoro-2-(2,2,2-trifluoro-1-thiomorpholinoethyl) aniline (41). Yellow oil (47% yield). ^1H NMR (400 MHz, CDCl_3), δ ppm = 7.07–7.03 (m, 1H), 6.43–6.37 (m, 2H), 4.66 (s broad, 2H), 4.48 (q, 1H, $J = 8.3$ Hz), 2.98–2.89 (m, 4H), 2.72–2.65 (m, 4H). ^{13}C NMR (400 MHz, CDCl_3), δ ppm = 164.01, 161.57, 161.42, 148.17, 130.62, 130.50, 111.73, 104.21, 103.83, 63.33, 62.80, 52.82, 27.68. LRMS ($\text{M} + \text{H}$) $^+$ (ESI $^+$) 295.08 [$\text{M} + \text{H}$] $^+$ (calcd for $\text{C}_{12}\text{H}_{15}\text{F}_4\text{N}_2\text{S}^+$ 295.09).

N-(1-(2-amino-6-fluorophenyl)-2,2,2-trifluoroethyl)-4-fluoroaniline (42). Brown oil (77% yield). ^1H NMR (400 MHz, CDCl_3) δ ppm = 7.14–7.08 (m, 1H), 6.91–6.87 (m, 2H), 6.69–6.67 (m, 2H), 6.59–6.51 (m, 2H), 5.32 (q, 1H, $J = 8.3$ Hz). ^{13}C NMR (100 MHz, CDCl_3) δ ppm = 170.28, 160.92, 158.15, 147.15, 142.06, 130.84, 130.73, 116.04, 115.81, 115.75, 115.68, 114.20, 114.17, 106.69, 106.65, 106.41, 54.52, 54.25, 54.19. LRMS ($\text{M} + \text{H}$) $^+$ (ESI $^+$) 302.98 [$\text{M} + \text{H}$] $^+$ (calcd for $\text{C}_{14}\text{H}_{12}\text{F}_5\text{N}_2^+$ 303.1).

MIC determination. *M. tuberculosis* H37Rv (ATCC 27294) was grown in either (1) 7H9/ADC/Tw consisting of Middlebrook 7H9 media (BD) supplemented with 0.5% BSA fraction V, 0.08% NaCl, 0.2% glucose, 0.05% Tween 80, and 0.2% glycerol; (2) GAST/Fe media consisting of 0.03% Bacto Casitone (Difco), 0.4% dibasic potassium

phosphate, 0.2% citric acid, 0.1% L-alanine, 0.12% magnesium chloride hexahydrate, 0.06% potassium sulfate, 0.2% ammonium chloride, 1% glycerol, 0.005% ferric ammonium citrate and 0.05% Tween 80 with pH adjusted to 6.8 with sodium hydroxide; or (3) 7H9/DPPC/casitone/Tx consisting of Middlebrook 7H9 media (BD) supplemented with 0.03% Bacto Casitone (Difco), 0.08% NaCl, 0.05% Tyloxapol and 14 µg/mL DPPC. Cultures were grown to OD_{650nm} of 0.2 and subsequently diluted 1:1000 in the same media. An equal volume of diluted cells (50 µL) was added to each well of clear round-bottom 96-well plates (Nunclon) containing compound serially diluted in the respective media (50 µL/well) in a concentration range spanning from 50 µM to 0.024 µM. Positive and negative controls were isoniazid and DMSO, respectively. Each compound serial dilution was tested in duplicate for each condition tested. The plates were incubated in sealed ziplock bags at 37 °C for 1 and 2 weeks at which time points growth was monitored with an enlarging inverted mirror. The MIC was recorded as the concentration of compound that resulted in complete inhibition of visual growth.

Cytotoxic activity assays. Vero cells were grown and maintained in RPMI 1640 medium supplemented with 2 mM of L-glutamine and 10% FCS. Cells were seeded in 96-well plates at a density of 1×10^4 cells/well. After 24 h, medium was replaced with fresh medium containing decreasing concentrations of the tested compound and incubated at 37 °C in 5% CO₂. Morphological changes were observed at 24, 48 and 72 h of incubation. The effects on the proliferation of Vero cells were determined after 72 h by tetrazolium-based colorimetric MTT assay. The 50% cell-inhibitory concentration (CC₅₀) reduced by 50% the optical density values (OD_{540,690}) with respect to control no-drug treated cells.

Bacterial strains and culture conditions. *M. bovis* BCG strains were grown in Middlebrook 7H9 media (BD) with 10% OADC culture supplement (BD), 0.025% Tween 80, and 0.2% glycerol, or on Middlebrook 7H10 agar (BD) with 10% OADC culture supplement (BD) and 0.2% glycerol. When needed, kanamycin was added to a final concentration of 25 µg/ml. To make BCG strains for inducible repression of the *trp* genes, primer pairs described in Supplemental Table 1 were annealed and ligated into BsmB-I linearized pJR962, as previously described [26]. The resultant plasmids (Supplemental Table 1) were verified by Sanger sequencing and transformed into wild type BCG by electroporation [29]. Three colonies from each transformation were picked and cultured in 7H9 broth supplemented with kanamycin.

Isolation of *M. bovis* BCG mutants resistant to 38 and 6-FABA. Mycobacterial strains were grown in Middlebrook 7H9 broth (Becton Dickinson) supplemented with 0.05% Tween 80 and 10% (vol/vol) albumin-dextrose-catalase (ADC) enrichment (Becton Dickinson). Mycobacterial cultures were grown at 37 °C with shaking for about one week, until reached exponential growth phase (OD₆₀₀ = 0.4–0.5). Compounds 38 and 6-FABA were dissolved in dimethyl sulfoxide. Cultures were diluted to the final concentration of about 10⁷ CFU/ml and 1 µl of dilutions and then streaked onto plates containing 2-fold scalar dilutions of compounds 38 and 6-FABA. The MIC was defined as the lowest concentration of drug preventing bacterial growth. All experiments were repeated three times. *M. bovis* mutants resistant to compounds 38 and 6-FABA were isolated by plating about 10¹⁰ cells from wild-type cultures (OD₆₀₀ = 0.5–0.6) onto solid media containing different concentrations of each compound, ranging from 3 to 10-fold MIC for the wild-type strain. Plates were incubated at 37 °C for 4 weeks. The MIC of compounds 38 and 6-FABA for the isolated resistant mutants was evaluated three times.

Genome sequencing and assembly. DNA was extracted by the CTAB-lysozyme method [30]. Samples were sequenced on an Illumina HiSeq Rapid 2500 with a read length of 150 bp in paired-end

mode. Genome sequences were assembled by a comparative-assembly method [31]. Reads were mapped to the genome sequence of *M. bovis* AF2122/97 (NC_002945.3) as a reference genome using BWA [32]. Then, regions with indels or clusters of single nucleotide polymorphisms (SNPs) were identified and repaired by building local contigs from overlapping reads spanning such regions. Genome sequences were aligned using MUMMER v3 [31,33]. SNPs were extracted according to the following criteria: coverage $\geq 10\times$ (covered by at least 10 reads) with purity $\geq 70\%$ (conversion to non-reference nucleotide). SNPs in repetitive regions were filtered out (repetitive regions were defined as sites for which an overlapping 35 bp window matches elsewhere in the genome with at most 2 mismatches).

Compound 38 sensitivity examination of CRISPRi knock-down BCG. BCG strains containing CRISPRi plasmids, as specified in Supplemental Table 1, were grown to log phase (OD₆₀₀ \approx 0.4) in the absence of the inducer ATC (anhydrotetracycline, Sigma). Cultures were then split into two halves and treated with either DMSO or 200 ng/mL ATC for 24 h to allow the pre-depletion of target transcripts. After pre-depletion, cells were diluted and added to a 96 well plate containing liquid broth of various concentrations of compound 38. ATC (final concentration 200 ng/ml) or an equal volume of DMSO was added to wells with cells that were pre-treated with ATC or DMSO, respectively. The final optical densities (OD₆₀₀) of diluted cultures are approximately 0.005. After 5 days of growth at 37 °C with constant shaking, resazurin (Sigma) was added to the cultures at a final concentration of 0.002%. Resazurin reduction was carried out at 37 °C for 12 h. Absorbances at 570 nm (A₅₇₀) and 600 nm (A₆₀₀) were measured using a benchtop plate reader (TECAN, Spark 10 M). Normalized bacterial growth (Fig. 6 B–D) was calculated by firstly subtracting the baseline A₅₇₀/A₆₀₀ (the median of cell-free control wells) readings from each well, then normalizing the strain-wise data by the median A₅₇₀/A₆₀₀ values of drug free wells. Statistical analyses were carried out using the *stats* module of the python scientific library, *Scipy*.

Declaration of competing interest

The authors declare that they have no known competing financial interests or personal relationships that could have appeared to influence the work reported in this paper.

Acknowledgments

This work has been supported by the Italian Ministry of Education, Universities and Research - Dipartimenti di Eccellenza - L. 232/2016 and in part by the Division of Intramural Research of the NIAID/NIH.

Appendix A. Supplementary data

Supplementary data to this article can be found online at <https://doi.org/10.1016/j.ejmech.2021.113843>.

References

- [1] 9789240013131-eng.pdf. <https://apps.who.int/iris/bitstream/handle/10665/336069/9789240013131-eng.pdf>. (Accessed 1 July 2021).
- [2] D.A. Smith, T. Parish, N.G. Stoker, G.J. Bancroft, Characterization of auxotrophic mutants of *Mycobacterium tuberculosis* and their potential as vaccine candidates, *Infect. Immun.* 69 (2001) 1142–1150, <https://doi.org/10.1128/IAI.69.2.1142-1150.2001>.
- [3] C. Burke, K.A. Abrahams, E.J. Richardson, N.J. Loman, C. Alemparte, J. Lelievre, G.S. Besra, Development of a whole-cell high-throughput phenotypic screen to identify inhibitors of mycobacterial amino acid biosynthesis, *FASEB Bioadv* 1 (2019) 246–254, <https://doi.org/10.1096/fba.2018-00048>.
- [4] M. Berney, L. Berney-Meyer, *Mycobacterium tuberculosis* in the face of host-

- imposed nutrient limitation, *Microbiol. Spectr.* 5 (2017), <https://doi.org/10.1128/microbiolspec.TBTB2-0030-2016>, 10.1128/microbiolspec.TBTB2-0030-2016.
- [5] J.-H. Park, D. Shim, K.E.S. Kim, W. Lee, S.J. Shin, Understanding metabolic regulation between host and pathogens: new opportunities for the development of improved therapeutic strategies against *Mycobacterium tuberculosis* infection, *Front. Cell. Infect. Microbiol.* 11 (2021), <https://doi.org/10.3389/fcimb.2021.635335>.
- [6] Y.J. Zhang, M.C. Reddy, T.R. Ioerger, A.C. Rothchild, V. Dartois, B.M. Schuster, A. Trauner, D. Wallis, S. Galaviz, C. Huttenhower, J.C. Sacchettini, S.M. Behar, E.J. Rubin, Tryptophan biosynthesis protects mycobacteria from CD4 T-cell-mediated killing, *Cell* 155 (2013) 1296–1308, <https://doi.org/10.1016/j.cell.2013.10.045>.
- [7] S. Wellington, P.P. Nag, K. Michalska, S.E. Johnston, R.P. Jedrzejczak, V.K. Kaushik, A.E. Clatworthy, N. Siddiqi, P. McCarren, B. Bajrami, N.I. Maltseva, S. Combs, S.L. Fisher, A. Joachimiak, S.L. Schreiber, D.T. Hung, A small-molecule allosteric inhibitor of *Mycobacterium tuberculosis* tryptophan synthase, *Nat. Chem. Biol.* 13 (2017) 943–950, <https://doi.org/10.1038/nchembio.2420>.
- [8] A. Blumenthal, G. Nagalingam, J.H. Huch, L. Walker, G.J. Guillemain, G.A. Smythe, S. Ehrhart, W.J. Britton, B.M. Saunders, *M. tuberculosis* induces potent activation of Ido-1, but this is not essential for the immunological control of infection, *PLoS One* 7 (2012), e37314, <https://doi.org/10.1371/journal.pone.0037314>.
- [9] J.M. Collins, A. Siddiqi, D.P. Jones, K. Liu, R.R. Kempker, A. Nizam, N.S. Shah, N. Ismail, S.G. Ouma, N. Tukvadze, S. Li, C.L. Day, J. Rengarajan, J.C. Brust, N.R. Gandhi, J.D. Ernst, H.M. Blumberg, T.R. Ziegler, Tryptophan catabolism reflects disease activity in human tuberculosis, *JCI Insight* 5 (2020) 137131, <https://doi.org/10.1172/jci.insight.137131>.
- [10] T.S. Johnson, D.H. Munn, Host indoleamine 2,3-dioxygenase: contribution to systemic acquired tumor tolerance, *Immunol. Invest.* 41 (2012) 765–797, <https://doi.org/10.3109/08820139.2012.689405>.
- [11] T. Lassila, J. Hokkanen, S.-M. Aatsinki, S. Mattila, M. Turpeinen, A. Tolonen, Toxicity of carboxylic acid-containing drugs: the role of acyl migration and CoA conjugation investigated, *Chem. Res. Toxicol.* 28 (2015) 2292–2303, <https://doi.org/10.1021/acs.chemrestox.5b00315>.
- [12] C. Li, L.Z. Benet, M.P. Grillo, Studies on the chemical reactivity of 2-phenylpropionic acid 1-O-acyl glucuronide and S-acyl-CoA thioester metabolites, *Chem. Res. Toxicol.* 15 (2002) 1309–1317, <https://doi.org/10.1021/tx020013l>.
- [13] S.D. Barrett, A.J. Bridges, D.T. Dudley, A.R. Salties, J.H. Fergus, C.M. Flamme, A.M. Delaney, M. Kaufman, S. LePage, W.R. Leopold, S.A. Przybranowski, J. Sebolt-Leopold, K. Van Becelaere, A.M. Doherty, R.M. Kennedy, D. Marston, W.A. Howard, Y. Smith, J.S. Warmus, H. Tecle, The discovery of the benzhydroxamate MEK inhibitors CI-1040 and PD 0325901, *Bioorg. Med. Chem. Lett.* 18 (2008) 6501–6504, <https://doi.org/10.1016/j.bmcl.2008.10.054>.
- [14] L. Di, E.H. Kerns, Chapter 39 - prodrugs, in: L. Di, E.H. Kerns (Eds.), *Drug-like Properties*, second ed., Academic Press, Boston, 2016, pp. 471–485, <https://doi.org/10.1016/B978-0-12-801076-1.00039-3>.
- [15] J.Y. Gauthier, N. Chaurat, W. Cromlish, S. Desmarais, L.T. Duong, J.-P. Falgoutyret, D.B. Kimmel, S. Lamontagne, S. Léger, T. LeRiche, C.S. Li, F. Massé, D.J. McKay, D.A. Nicoll-Griffith, R.M. Oballa, J.T. Palmer, M.D. Percival, D. Riendeau, J. Robichaud, G.A. Rodan, S.B. Rodan, C. Seto, M. Thérien, V.-L. Truong, M.C. Venuti, G. Wesolowski, R.N. Young, R. Zamboni, W.C. Black, The discovery of odanacatib (MK-0822), a selective inhibitor of cathepsin K, *Bioorg. Med. Chem. Lett.* 18 (2008) 923–928, <https://doi.org/10.1016/j.bmcl.2007.12.047>.
- [16] S.G. Franzblau, M.A. DeGroot, S.H. Cho, K. Andries, E. Nuermberger, I.M. Orme, K. Mdluli, I. Angulo-Barturen, T. Dick, V. Dartois, A.J. Lenaerts, Comprehensive analysis of methods used for the evaluation of compounds against *Mycobacterium tuberculosis*, *Tuberculosis (Edinb.)* 92 (2012) 453–488, <https://doi.org/10.1016/j.tube.2012.07.003>.
- [17] S. Oh, Y. Park, C.A. Engelhart, J.B. Wallach, D. Schnappinger, K. Arora, M. Manikkam, B. Gac, H. Wang, N. Murgolo, D.B. Olsen, M. Goodwin, M. Sutphin, D.M. Weiner, L.E. Via, H.I.M. Boshoff, C.E. Barry, Discovery and structure-activity-relationship study of N-alkyl-5-hydroxypyrimidinone carboxamides as novel antitubercular agents targeting decaprenylphosphoryl- β -D-ribose 2'-Oxidase, *J. Med. Chem.* 61 (2018) 9952–9965, <https://doi.org/10.1021/acs.jmedchem.8b00883>.
- [18] S. Tafazoli, M. Mashregi, P.J. O'Brien, Role of hydrazine in isoniazid-induced hepatotoxicity in a hepatocyte inflammation model, *Toxicol. Appl. Pharmacol.* 229 (2008) 94–101, <https://doi.org/10.1016/j.taap.2008.01.002>.
- [19] S. Consalvi, C. Scarpecci, M. Biava, G. Poce, Mycobacterial tryptophan biosynthesis: a promising target for tuberculosis drug development? *Bioorg. Med. Chem. Lett.* 29 (2019) 126731, <https://doi.org/10.1016/j.bmcl.2019.126731>.
- [20] M. Nurul Islam, R. Hitchings, S. Kumar, F.L. Fontes, J.S. Lott, N.A. Kruh-Garcia, D.C. Crick, Mechanism of Fluorinated anthranilate-induced growth inhibition in *Mycobacterium tuberculosis*, *ACS Infect. Dis.* 5 (2019) 55–62, <https://doi.org/10.1021/acsinfecdis.8b00092>.
- [21] A.A. Morollo, M.J. Eck, Structure of the cooperative allosteric anthranilate synthase from *Salmonella typhimurium*, *Nat. Struct. Mol. Biol.* 8 (2001) 243–247, <https://doi.org/10.1038/84988>.
- [22] J.S. Lott, The tryptophan biosynthetic pathway is essential for *Mycobacterium tuberculosis* to cause disease, *Biochem. Soc. Trans.* 48 (2020) 2029–2037, <https://doi.org/10.1042/BST20200194>.
- [23] M.D.J. Libardo, C.J. Duncombe, S.R. Green, P.G. Wyatt, S. Thompson, P.C. Ray, T.R. Ioerger, S. Oh, M.B. Goodwin, H.I.M. Boshoff, C.E. Barry, Resistance of *Mycobacterium tuberculosis* to indole 4-carboxamides occurs through alterations in drug metabolism and tryptophan biosynthesis, *Cell. Chem. Biol.* (2021) S2451–S9456, <https://doi.org/10.1016/j.chembiol.2021.02.023>, 00108–2.
- [24] C.Z. Schneider, T. Parish, L.A. Basso, D.S. Santos, The two chorismate mutases from both *Mycobacterium tuberculosis* and *Mycobacterium smegmatis*: biochemical analysis and limited regulation of promoter activity by aromatic amino acids, *J. Bacteriol.* 190 (2008) 122–134, <https://doi.org/10.1128/JB.01332-07>.
- [25] A. Kapopoulou, J.M. Lew, S.T. Cole, The MycoBrowser portal: a comprehensive and manually annotated resource for mycobacterial genomes, *Tuberculosis* 91 (2011) 8–13, <https://doi.org/10.1016/j.tube.2010.09.006>.
- [26] J.M. Rock, F.F. Hopkins, A. Chavez, M. Diallo, M.R. Chase, E.R. Gerrick, J.R. Pritchard, G.M. Church, E.J. Rubin, C.M. Sasseti, D. Schnappinger, S.M. Fortune, Programmable transcriptional repression in mycobacteria using an orthogonal CRISPR interference platform, *Nat. Microbiol.* 2 (2017) 16274, <https://doi.org/10.1038/nmicrobiol.2016.274>.
- [27] S. Sasso, M. Okvist, K. Roderer, M. Gamper, G. Codoni, U. Krengel, P. Kast, Structure and function of a complex between chorismate mutase and DAHP synthase: efficiency boost for the junior partner, *EMBO J.* 28 (2009) 2128–2142, <https://doi.org/10.1038/emboj.2009.165>.
- [28] V. Singh, M. Brecik, R. Mukherjee, J.C. Evans, Z. Svetlíková, J. Blaško, S. Surade, J. Blackburn, D.F. Warner, K. Mikušová, V. Mizrahi, The complex mechanism of antimycobacterial action of 5-Fluorouracil, *Chem. Biol.* 22 (2015) 63–75, <https://doi.org/10.1016/j.chembiol.2014.11.006>.
- [29] R. Goude, T. Parish, Electroporation of mycobacteria, in: T. Parish, A.C. Brown (Eds.), *Mycobacteria Protocols*, second ed., Humana Press, Totowa, NJ, 2009, pp. 203–215, https://doi.org/10.1007/978-1-59745-207-6_13.
- [30] M.H. Larsen, K. Biermann, S. Tandberg, T. Hsu, W.R. Jacobs, Genetic manipulation of *Mycobacterium tuberculosis*, *Curr. Protoc. Microbiol.* Chapter 10 (2007), <https://doi.org/10.1002/978047129259.mc10a02s6>, Unit 10A.2.
- [31] T.R. Ioerger, Y. Feng, K. Ganesula, X. Chen, K.M. Dobos, S. Fortune, W.R. Jacobs, V. Mizrahi, T. Parish, E. Rubin, C. Sasseti, J.C. Sacchettini, Variation among genome sequences of H37Rv strains of *Mycobacterium tuberculosis* from multiple laboratories, *J. Bacteriol.* 192 (2010) 3645–3653, <https://doi.org/10.1128/JB.00166-10>.
- [32] H. Li, R. Durbin, Fast and accurate long-read alignment with Burrows-Wheeler transform, *Bioinformatics* 26 (2010) 589–595, <https://doi.org/10.1093/bioinformatics/btp698>.
- [33] S. Kurtz, A. Phillippy, A.L. Delcher, M. Smoot, M. Shumway, C. Antonescu, S.L. Salzberg, Versatile and open software for comparing large genomes, *Genome Biol.* 5 (2004) R12, <https://doi.org/10.1186/gb-2004-5-2-r12>.